Developments in Fish Detection using Broadband Acoustic Doppler Current Profiler

by

© Muriel Dunn

A thesis submitted to the

School of Graduate Studies

in partial fulfilment of the

requirements for the degree of

Master of *Science*

Department of Physics and Physical Oceanography

Memorial University of Newfoundland

October 30, 2019

St. John's Newfoundland

Abstract

Acoustic Doppler current profilers (ADCPs) are the standard instrument used to monitor ocean currents. These instruments also detect signals scattered by fish and other organisms, but these signals are normally treated as noise and rejected by ADCP data processing techniques. Those rejected signals do however contain information on fish movement providing an opportunity to extend the application of ADCP technology. The added capability of the ADCP offers a monitoring tool for fish activity and presence in areas that may be impacted by future in-stream hydro energy development projects. We explore this capability through two deployments, 37 days and 28 days, of a self-contained bottom-mounted frame equipped with a 600 kHz RD Instruments Workhorse ADCP alongside a 120 kHz BioSonics DTX Submersible Split-Beam Echosounder system. The deployments took place in Grand Passage, Nova Scotia, a tidal channel that has the potential for in-stream tidal generation. The split-beam echosounder's dataset shows plumes of scatterers, presumably entrained air, emanating from the surface. Discrete fish targets were detected throughout the water column within dense schools and as individuals. The corresponding ADCP data detects the same fish schools by using coincident incidences of high intensity and high signal correlation. A common problem for fish detection in high energy tidal channels is entrained air (i.e. bubbles plumes). I show that fish can be differentiated from entrained air using a high signal correlation threshold with the broadband ADCP. This thesis presents results from both instruments and contrasts their capabilities in the context of fish monitoring in high-energy tidal channels.

Acknowledgements

My research supervisor, Dr. Len Zedel, has been integral throughout this research. Dr. Zedel has educated me on ocean acoustics while increasing my curiosity to learn more about it. Additionally, he has taught me to be a more assertive and effective researcher.

Greg Trowse at Luna Ocean Ltd. has provided an unparalleled expertise of the research site and its communities. Mark Downey, from Memorial University of Newfoundland, provided instrumentation knowledge for the deployments and the lab tests. Richard Cheel from Dalhousie University has been invaluable help in the field.

I thank the two reviews for their comments and suggestions on this manuscript.

This work was funded by the Nova Scotia Offshore Energy Research Association.

Contents

List of Tables

List of Figures

Chapter 1

Introduction

1.1 Motivation for research

The use of acoustics in fisheries research for abundance estimates is critically important. Acoustic surveys can collect data with high spatial and temporal resolution in areas where trawl sampling is difficult and they are a non-invasive survey method. As a research tool, acoustic surveys provide information and measurements on marine life, ranging from mammals to zooplankton. Reliable abundance and distribution measurements are particularly important in light of rapidly changing ocean temperatures, marine habitats and fish stocks. Acoustic surveys provide a much-needed method to assess aquatic populations through large volumes of water. Acoustics for fisheries research is often combined with direct sampling methods, such as trawl sampling or video for ground-truthing and species identification [Foote et al., 1986, Broadhurst et al., 2014, Viehman and Zydlewski, 2015]. Conventionally, ships undertake acoustic surveys for fish populations on a prescribed survey

pattern over an area of interest. These surveys provide a snapshot in time of the distribution of fish. Repeat surveys are necessary to monitor the change in fish population over time. This surveying process is time-consuming and, perhaps more critically, very expensive because of the cost of operating a survey ship.

Currently, the industry standard for fish detection are split-beam echosounders. In ideal survey conditions, their echograms provide a clear image of fish as they travel through the beam of ensonified water. For high-energy tidal channels, the conventional processing approach is to limit the depth range by excluding the surface as it is difficult to distinguish bubbles from fish in areas of entrained air [Staines et al., 2015]. When fish form dense aggregations, it can be difficult to acoustically identify an individual fish from its neighbour when the signal is over-saturated. To resolve the over-saturation of the signal in fish schools, a standard approach is to omit fish schools from the analysis [Viehman and Zydlewski, 2017]. Specialized processing methods have been developed in response to these gaps in data, but they require an in-depth prior knowledge of the site dynamics and the targeted species behaviour [Fraser et al., 2017]. Fisheries echosounders are traditionally designed for hull-mounted and coastal surveys which rely on good weather and calm waters because in rough seas the pitch and roll of the boat can make the acoustic instruments survey at inconsistent angles. On the other hand, bottom-mounted moored sounders collect data regardless of weather, therefore provide valuable information in turbulent waters.

In this thesis, a new approach to monitor fish presence is explored through the use

of long-term bottom-mounted and upward-looking observations. The new approach is intended to complement existing acoustic survey methods. An important component of this research is fish detection. The approach used will expand the capability of the broadband Acoustic Doppler current profilers (ADCPs) which is the standard instrument used to monitor ocean currents. While researchers have suggested using ADCP's for fisheries studies, they have encountered processing and technology advancement issues with algorithm developments and calibration ([Holliday, 1977], [Olsen et al., 1983] [Demer et al., 2000]). These findings are addressed in Chapter 2.2.

Doppler Profilers have been used extensively since the mid 80's to measure flow speeds. These instruments inevitably detect signals scattered by fish but those fish signals are normally treated as noise and rejected by conventional ADCP data processing techniques. Those rejected signals do however contain information on fish presence and movement providing an opportunity to extend the application of ADCP technology. Zedel and Cyr-Racine (2009) proposes a least-squares approach to Doppler signal processing to distinguish discrete (fish) targets from ocean volume backscatter. That capability will allow long-term monitoring of fish movement at one location in the context of ocean currents, similar to the ship avoidance work from Ona et al. (2007). However, the method still needs to be validated with the industry standard for fish detection.

In the context of this thesis, an experiment was designed to validate the algorithm. An ADCP was deployed beside a split-beam echosounder so that fish counts from the

two instruments could be compared. The availability of collocated data made it possible to establish optimal processing approaches with the new ADCP least-squares algorithm.

The objective of the deployment of collocated instruments is to answer the following questions:

1. Can an ADCP accurately detect fish?
2. Can techniques used to detect fish in ADCP data complement and improve current fish detection methods?
3. Can this fish detection algorithm calculate fish counts in other ADCP datasets?

The developments that are proposed here will extend the present measurement capability of fisheries research by enabling long time records of fish movement. This approach will offer a time series view of fish presence complementary to traditional ship surveys of fish abundance. For the specific case of in-stream tidal developments, the observations will provide a record of fish environmental response to turbines. This information is crucial in sustainably maintaining fish populations as the tidal energy industry grows. The methods developed can also be applied more generally to studies of fish abundance or assessments where movement or evolution over time is of particular interest.

1.2 Thesis Overview

This thesis is composed of 6 chapters. The literature review in Chapter 2 summarizes the use of sonars for ocean research with a detailed focus on ADCPs and split-beam echosounders. This chapter also gives an overview of previous research on the use of ADCPs for fish detection. The current state of the knowledge of the effect of in-stream tidal turbines on individual fish behaviour and fish populations is explored. We also identify existing knowledge gaps that could be resolved with ADCPs for fish detection, for example in high-energy channels identified as tidal energy extraction sites. Chapter 3 describes the experimental methods used to execute a month-long direct comparison of two collocated acoustic instruments in a high-energy tidal channel. The strategies addressed are the duty cycle choices due to the chance of interference between instruments, data collection settings and calibrations. We also discuss battery consumption and the methods used to calculate a robust operating life estimates for the split-beam echsounder. Chapter 4 provides an in-depth account of the computational methods used to analyze the datasets. The methods used to determine the thresholds and parameters for both instruments are explained. This chapter also explains the development and improvement work done with the Broadband Acoustic Monitoring For Fish (BAMFF) package [Zedel et al., 2019]. Chapter 5 examines the results of the comparison between the split-beam echosounder and the ADCP. The results compare and contrast both instruments abilities for fish detection and discuss the results of target strength and detection in entrained air. The final chapter of this thesis, Chapter 6, summarizes the work and places it in context with its relevance to the field. The future of fish detection and an outlook on extracting fish velocities

using broadband ADCPs is addressed.

Chapter 2

Literature Review

This chapter provides background theory on sonars. It overviews the research that has shaped the current state of fish detection with ADCPs. It includes an in-depth comparison of the methods used by split-beam echosounders and their limitations. To contextualize, the application of fish detection at sites of tidal-energy extraction is explored through the knowledge gaps of the effect of tidal turbines on fish behaviour.

2.1 Sonars

Sonars are used for detection and to remotely measure objects in the ocean. Generally, active sonars use a transmitter to generate an electrical signal at a particular frequency which is converted into a sound by a transducer. The sound forms a beam of sound through the water column away from the face of the transducer. These propagating sound waves are scattered by any object with an acoustic impedance different than the medium through which the sound is travelling. The transducer receives the scattered signal that is returned towards the instrument. The instrument amplifies

the received signal and converts it from analogue to digital for further processing. These basic concepts are modified for a variety of different applications, for example, water velocity extraction and fisheries sciences. The differences that distinguish the sonars used in these fields are described below.

Water velocity studies have applications for measuring the velocity of a ship relative to the seafloor, ocean surface speed, internal waves or currents. These applications use Doppler sonars, more specifically ADCPs. These instruments are described in more detail in Chapter 2.2.

Fisheries acoustics mainly uses echosounders. They are a specific type of sonar in which the system is designed to detect and observe fish or the depth of the seabed. Acoustics is prevalent in fisheries research; in part because fish swim bladders are an effective target because the acoustic impedance of air and water differ greatly from each other and in part because fisheries acoustics provides a non-invasive survey method [Trenkel et al., 2019]. In the most basic single-beam echosounders, e.g. fish finders, fish schools can be identified, but there is no way to differentiate a small fish in the middle of the beam from a large fish on the edge of the beam, therefore target strength cannot be quantified. Target strength (TS) is used by bioacousticians to quantify the size of echoes to learn as much as possible about fish populations [Medwin and Clay, 1997].

2.1.1 Sonar Equation and Target Strength

Target strength can be put into context through the log-sonar equation, Equation 2.1 [Medwin and Clay, 1997], which is used to measure the sound pressure received by the transducer, represented as sound pressure level, SPL.

$$SPL = SL - 2TL + TS \tag{2.1}$$

$$SPL = 20\log_{10}(\frac{P_{bs}}{P_{ref}}) \tag{2.2}$$

$$SL = 20\log_{10}(\frac{P_0}{P_{ref}}) \tag{2.3}$$

The SPL, Equation 2.2, is the sound pressure backscattered to the instrument, P_{bs}, in logarithmic terms. It is based on on the emitted signal level, SL, the sound pressure at the source, P_0, in logarithmic terms, Equation 2.3, transmission loss, TL, which is the sound lost due to range and absorption, and target strength, TS. All of these terms are measured in decibels. The sound level and sound pressure level are calculated from their linear pressure levels relative to a reference pressure, P_{ref}, 1 μPa in the ocean.

$$TL = -20\log_{10}(\frac{R}{R_0}) + \alpha R \tag{2.4}$$

.

The transmission loss term encompasses much of the complexities involved in underwater acoustic propagation. It is dependent on bathymetry, sound speed profiles, multipath arrivals, range, source frequency, divergence from the source to receiver,

absorption and scattering [Medwin and Clay, 1997]. Much of that complexity is hidden in the absorption loss term, α, in $\frac{dB}{m}$, within Equation 2.4, but it is also a function of the range of the target, R, and the reference range, R_{ref}, 1 m in ocean acoustics. Here we describe transmission loss for spherical spreading, as opposed to cylindrical spreading, because it is appropriate for propagation in the case where sound does not interact with the ocean boundaries.

The last item in the sonar equation, Equation 2.1, is target strength, TS. It describes the fraction of incident acoustic energy scattered back to the instrument. TS is measured by converting the backscattering cross-section (σ_{bs}) of a target to a logarithmic scale:

$$TS = 10 \log_{10}(\sigma_{bs}) \tag{2.5}$$

$$\sigma_{bs} = V * s_v \tag{2.6}$$

where V is the sampled volume and the volume backscatter coefficient is s_v, in m^{-1} [Maclennan et al., 2002]. The volume backscatter coefficient is the linear measure of the logarithmic volume backscatter strength S_v:

$$S_v = 10 \log_{10}(s_v) \tag{2.7}$$

The volume backscatter strength, S_v, is commonly used to demonstrate the received signal in dB re 1 m^{-1} [Maclennan et al., 2002].

The sample volume is a measure of the space that contributes echoes to the transducer for any signal [MacLennan and Simmonds, 2013] it can be related to the acoustic beam pattern as:

$$V = \frac{c\tau\psi R^2}{2} \tag{2.8}$$

where the range is R, the pulse length is τ and the sound speed velocity is c. The sample volume represents a measure of the beam width [MacLennan and Simmonds, 2013] and results in the direction of the target relative to the origin of the transducer. The equivalent beam angle, ψ, indicates the solid angle of an idealized acoustic beam:

$$\psi = \int_{\theta=0}^{\pi} \int_{\phi=0}^{2\pi} b^4(\theta, \phi) \mathrm{d}\theta \mathrm{d}\phi. \tag{2.9}$$

where for an ideal cylindrical transducer, the directivity is expressed as:

$$b = \frac{2J_1(ka\sin(\theta))}{ka\sin(\theta)} \tag{2.10}$$

where the transducer radius, a, wavenumber, k and J_1 is a Bessel function of the first kind [Medwin and Clay, 1997].

When combined with knowledge of the study site and the expected species, target strength can provide an indicator of fish species, size and biomass estimates [MacLennan and Simmonds, 2013] because it reports the size of the echo. When this type of data is used to determine the length dependence on target strength, the TS-length relationship, it can be very powerful for extrapolating existing datasets of target strength and population [Foote et al., 1986]. Target classification, such as species

identification based on TS-length relationship and frequency, is an active research topic [Korneliussen, 2018] because it could decrease the need for complementary trawl surveys in areas where species composition is not well understood. However, having the equations is not enough; the instruments must be able to provide a calibrated and precise volume backscatter and range measurement of the targets. For a meaningful target strength result, echosounder technology has gone through decades of iterations to provide a calibrated target strength, for example, from narrowbeam to split-beam, in parallel, the required calibration protocols have been established.

2.1.2 Echosounders

Many types of echosounders have been developed with increasing complexities to improve on some of the drawbacks of single-beam echosounders, such as to correct for the effect of the beam pattern from an acoustic echo [Ehrenberg and Torkelson, 1996]. Dual-beam and split-beam echosounders are designed to improve direct *in situ* target strength measurements [MacLennan and Simmonds, 2013]. Dual-beam echosounders are composed of center elements that form and widebeam and outer elements that form a narrowbeam. The received signal of the wide and narrow beam are compared to determine backscattering cross-section, range and off-axis location of targets by calculating the ratio of the intensity of their received signals. Dual-beam echosounders are more affected by additive noise compared to split-beam echosounders because they have a lower signal to noise ratio [Ehrenberg and Torkelson, 1996]. For this reason alone, dual-beams systems are inferior to split-beam echosounders [Foote et al., 1986].

Additionally they do not provide angular location [Ehrenberg and Torkelson, 1996]. Therefore, we focus on split-beam echosounders as the industry standard for fisheries acoustics, described in Section 2.3; these instruments provide information on swimming speeds, location in the water column and the direction of travel of individual fish [Ehrenberg and Torkelson, 1996], all of which are useful to study fish behaviour.

Formalizing the additional capability of the ADCP to detect fish would complement present methods used for fisheries sciences. In this thesis, we made a direct comparison of the industry standard for fisheries acoustic studies, split-beam echosounder with an ADCP for fish detection.

2.2 Acoustic Doppler Current Profiler

For most echosounders, the scattered signal will be received through the same transducer that emitted the original sound pulse. In the case of ADCPs, the standard instruments for measuring ocean current velocities, the sound pulses are emitted and received through four narrow beam transducers (about 4° to the -3 dB point on the beam) each directed 20° from the vertical. Each transducer emits a pulse of a known frequency which gets scattered by suspended particles in the water column. The energy that is scattered back to the instrument is described as being backscattered. The frequency of the backscattered signal is shifted in proportion to the velocity of the scatterer by the process of Doppler shifting. Based on the frequency shift in each beam, the ADCP can calculate the radial velocity of the scatterers. The change in frequency due to the Doppler effect, is given by:

$$f_r = f_0 - \frac{2v_R f_0}{c} \tag{2.11}$$

where v_R is the radial component of the relative velocity between the source and the scatterer, c is the speed of sound in water, f_0 is frequency emitted by the source, f_r is the frequency received [MacLennan and Simmonds, 2013]. The factor of 2 is due to the moving target's velocity relative to the source shifting the frequency twice; once, when the sound is received by the moving target and a second time, when it returns to the source.

Each transducer provides the component of velocity along its beam axis; traditionally, the result of each beam is grouped into depth bins and is combined with the other beams to provide the velocity as a profile of three component velocity vector. This method assumes that flow is homogeneous between the beams and within the whole depth bin, as shown in Figure 2.1.

Even though the principle is the same for all types of Doppler instruments, they vary in the way they transmit the signal. Narrowband ADCPs send a long pulse of acoustic energy with a known frequency and calculates the frequency of the echo; the along-beam velocity is determined by comparing the difference in sent and received frequencies. The pulse must be long in order to establish a specific known frequency, the longer the pulse the less it will include other frequencies. Incidentally, a long pulse will cause the water profile to be averaged into large depth bins, resulting in poor depth resolution. A narrowband ADCP has a limited precision because the

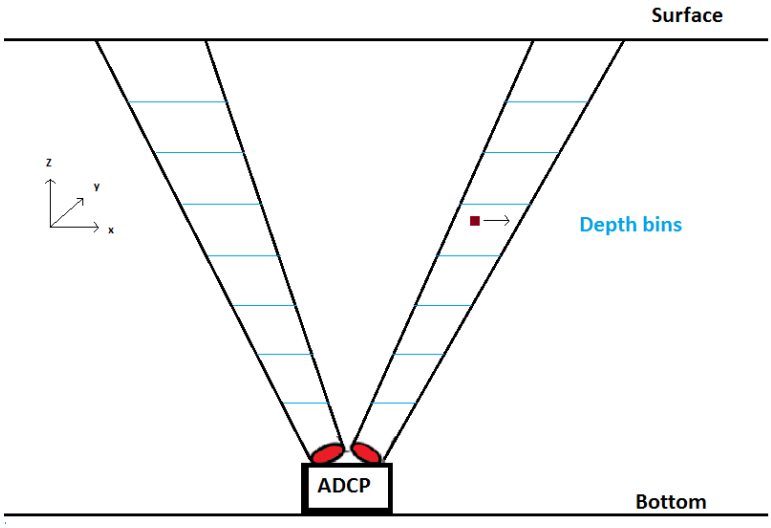

Figure 2.1: Bottom-mounted ADCP with the depth bins shown. The cube is a passive target following the water flow, such as biota or sediment.

pulse length and depth bins are interrelated. Coherent systems send two pulses but wait to have received the echo of the first pulse before sending the second pulse, which can create a relatively long lag between pulses. The phase shift between the pulses is analyzed to calculate the water velocity, the long lag provides a more precise measurement. However, if the lag is too long, relative to the water velocity, the pulses won't be measuring the same parcel of water, which leads to a decorrelation of the pulses. Even if the pulses are correlated, if the velocity is too great, the phase difference becomes too large and causes a phase wrap. The phase wrap is explained through the ambiguity velocity.

Ambiguity velocity arises from using the phase difference between the pulse pair to calculate velocity. As the velocity increases and the phase difference wraps past $\pm\pi$, a new velocity range is started without indication to which velocity range the phase difference corresponds. The maximum velocity in the lowest velocity domain determines the ambiguity velocity, or the maximum velocity that can be resolved.

Broadband systems send pulse pairs with a lag between them. The water velocity is proportional to the phase difference between the echoes of the pulse pair, which is detected through the auto-correlation of the received signal. In this thesis, the signal auto-correlation is used to differentiate fish from incoherent targets, such as entrained air. This type of Doppler system is 20 years old (1995), it is essentially a coherent system that accepts range ambiguity associated with having two pulses in the water column at the same time. It overcomes this problem by using a large bandwidth to make many independent estimates of velocity. Ambiguity velocity is a concern with

broadband as well as coherent ADCPs.

Signals received by ADCPs contain backscatter from a variety of objects in the water column, including fish, zooplankton, sediments, bubbles and the surface or bottom. As the instrument is used for water velocity measurements, typically all signals that differ significantly in echo intensity between the four beams are rejected to reduce fish bias in velocity data [Freitag et al., 1993]. The significant difference in echo intensity suggests that one beam is detecting something different from the other beams (i.e. a fish). This is the basis utilized by the rejected fish signals as a data source to study fish.

Vent et al. (1976) works on using Doppler measurement for determining the target strength of entire fish schools. Only the radial velocities were resolved because there was no homogeneity within each depth bin. Vent concludes that the interaction between acoustic energy and fish schools is very complex and dependent on the physical and acoustical properties of the observed school [Vent et al., 1976].

Holliday (1977) states, "...the utilization of measurements involving the Doppler phenomenon can play a valuable role in the study of fishery resources" on using the Doppler effect for his study of fish schools dynamics relative to water and to study movement within a fish school. Holliday's work is done using a narrowbeam ADCP with a long pulse length.

Olsen et al. (1983) compares video, echosounder and Doppler shift measurements

to measure velocity estimates of herring and cod as a function of vessel speed to quantify fish reaction to a surveying vessel. The speed of the vessel and the depth of the fish are found to be important in identifying the magnitude of the velocity of the fish schools. The echosounder limitations are observed when recording groups of fish that are not sufficiently dispersed to allow for single-target echo detection. Olsen et al. (1983) suggests that studies on the behaviour of dense fish aggregations could benefit from Doppler shift measurements because it could provide velocity measurements through the fish echoes recorded.

Most research methods before Demer (2000) use low frequency, long pulses and narrow bandwidth. Though Doppler shift methods were promising, theoretically, for gathering information on fish behaviour, the equipment settings and data processing algorithms were not fully developed. Demer (2000) suggests that ADCPs need to achieve higher velocity and range resolution and shows that this could be accomplished by using a higher frequency, and auto-correlation for the detection of pulse shifts. Demer (2000) also identifies a need to modify data collection parameters and data processing as well as to select survey sites carefully with fish schools matched to the size of the processing bins.

2.2.1 Velocity measurements

Conventional processing methods for water velocity extraction with Doppler profilers combine the radial velocity of each beam to resolve the velocity vector of the passive

sediment and biota targets. This method requires all the beams to be detecting the same homogeneous flow within each depth bin. Fish targets and other targets that "corrupt" the signal by having an anomalous volume backscatter are rejected from the calculation.

Zedel and Cyr-Racine (2009) present an alternative approach to analyzing Doppler sonar data using a least-squares based algorithm which treats each acoustic beam individually to extract both fish and water velocities, even when fish are intermittently present. The main difference is that their optimization algorithm utilizes all the data collected by the Doppler profiler rather than only using data for which the assumptions of homogeneous flow over the beam sample volumes can be assured. All observations are identified as fish or water targets and are binned by time and depth intervals; these subsets are used to determine the velocity of water and fish (if present) in that bin.

If the measured velocity is $\vec{V} = \{V_x, V_y, V_z\}$ and the unit vector that describes the orientation of the j'th component measurement is $\hat{k}_j = \{k_{xj}, k_{yj}, k_{zj}\}$. We can express the best choice of velocity as,

$$v_j = \vec{V} \cdot \hat{k}_j = V_x k_{xj} + V_y k_{yj} + V_z k_{zj} \tag{2.12}$$

If there is enough measurements within a range of orientations, a standard least-squares approach can be used to minimize the sum of the square of the residuals between the measured velocities and predicted v_j. By doing this for all observations,

the optimal x, y and z component of the velocity vector will be extracted. This is beneficial because it bypasses the dependency on a homogeneous flow and accommodates mixing missed and rejected data [Zedel and Cyr-Racine, 2009].

This method is more computationally involved but provides more information. The algorithm has been validated for water velocity measurements through a field test and provides the same velocity results as the standard Doppler processing method [Zedel and Cyr-Racine, 2009]. The velocity of fish relative to the water velocity differentiates a small stationary school from a large transient swimming school. Even with a suitable processing algorithm for fish velocity extraction, the challenge remains to identify the presence of fish in ADCP data accurately.

2.2.2 Calibration

Doppler profilers, like any other acoustic instrument, must be routinely calibrated to account for the offset in intensity of the signal. Each beam of the ADCP is calibrated for sensitivity by finding the slope of the echo intensities. The echo intensity is required for volume backscatter measurements, S_v, because it describes the reflective characteristics of sound. The calibration is performed by transmitting a known frequency to the transducer of the ADCP by acoustically coupling another transducer to its face. The signal is incrementally decreased; the corresponding measured echo intensity voltage is measured and recorded [McTamney, 2019]. The slope, in counts/dB, of these measurements is calculated for each beam to determine the sensitivity.

2.3 Fish tracking with split-beam echosounders

Split-beam echosounders send an acoustic pulse through the water column, like a conventional (single-beam) transducer but the transducer receives the backscatter in 4 separate quadrants. If the target is on-axis, in the middle of the beam, all the quadrants will receive the signal with the same phase. As the target ventures off the center axis, the phase difference between the signal from each quadrant is used to locate the target in the beam, as shown in Figure 2.2. When combined with the on-axis sensitivity and the beam pattern of the echosounder, the location of the target in the beam is used to determine absolute target strength. The variance of the average target strength can be significantly reduced by using the method of target tracking. Tracking provides multiple estimates of the target strength for a single fish; the reduced TS variance leads to better size estimates and species identification [Ehrenberg and Torkelson, 1996].

Target tracking provides a better estimate of target strength and extracts fish velocity relative to the echosounder for individual fish targets. A variety of algorithms have been developed with varying complexity to identify and isolate a single fish and follow it through time and space as it swims through the beam. Algorithms differ in the way they address the challenges imposed by the survey site or the species. Common challenges are large swim speed, TS changing with fish tilt angle, entrained air and fish swimming in and out of the beam. Some algorithms have been designed to improve on certain challenges, for example, Balk's cross-filter detector minimizes signal contamination [Balk and Lindem, 2017] and Fraser's algorithm focuses on de-

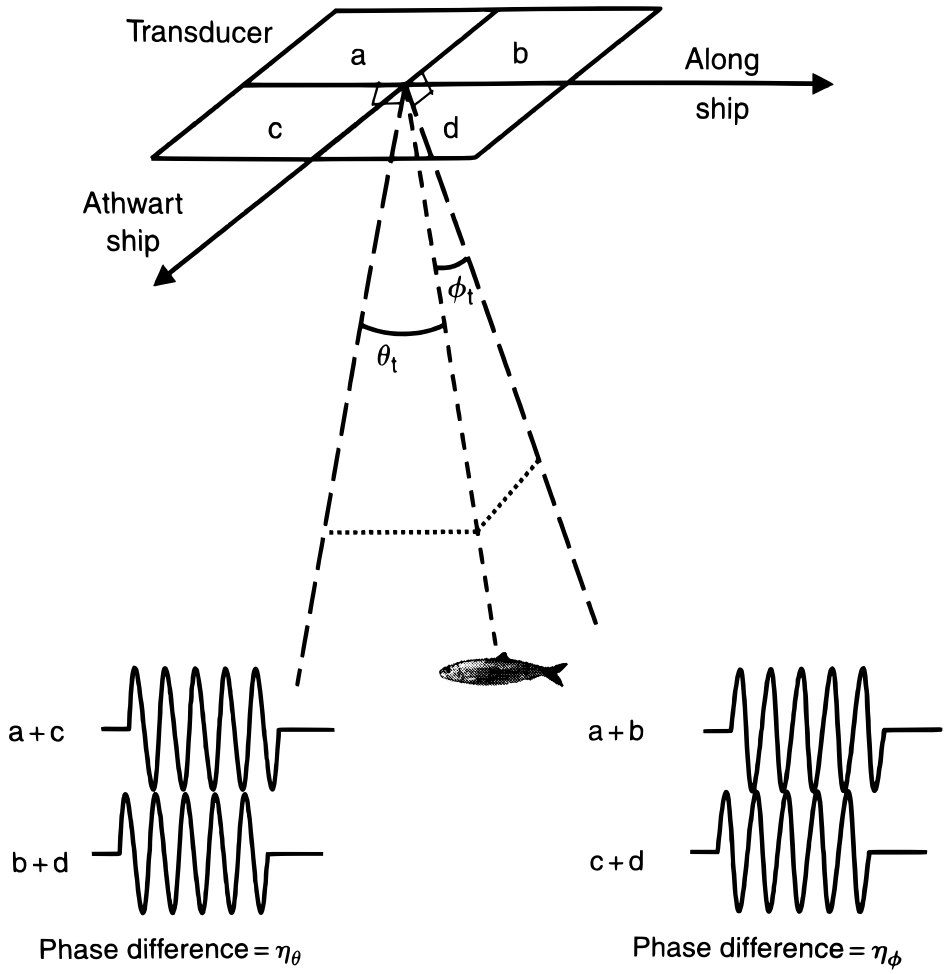

Figure 2.2: A split-beam echosounder diagram with its four quadrants and the phase difference analysis used to locate the fish in the beam. An image from [MacLennan and Simmonds, 2013]. Permissions by John Wiley & Sons Company.

tecting fish targets in highly turbulent areas [Fraser et al., 2017]. However, all of the target tracking algorithms require careful setup and in-depth knowledge of the target species [Xie et al., 1997]. Adequate setup can be labour intensive because the target tracking algorithm parameters must be tuned specifically for the study site and its scatterers.

Target tracking requires many post-processing steps but significantly increases the amount of information provided by a split-beam echosounder. When fish aggregations are too dense, individual fish echoes cannot be isolated, and the fish tracking algorithm is unable to create individual fish tracks to extract swim speeds and averaged target strengths. The best results for fish tracking are achieved when the mean density of fish is low, and the target strength distribution width is narrow. A low fish density minimizes the chances of detecting echoes from two or more fish as a single target, resulting in data which be discarded. When multiple species are present, additional processing steps are required to identify single targets due to their respective target strength values [MacLennan and Simmonds, 2013]. A narrow TS distribution allows the user to select species specific parameters. Carefully chosen parameters with narrow ranges for the minimum and maximum values facilitate fish identification and can reduce the detection of false targets.

For the purpose of echo counting if fish aggregations are too dense, a method called echo integration can be used to estimate the biomass of fish in the acoustic beam regardless of the signals overlapping. Echo integration is a well-established technique for estimating biomass or target density. The total echo intensity over a

prescribed sample volume is used to calculate the density of a group of targets. Echo integration relies on the linearity of the echo energy, which means that the echo energy of a school of fish is the sum of all the individual contributions of the echo energy of each fish [Foote, 1983]. The fish counts can be estimated from the target density if the mean target density of the population is known.

Enzenhofer's experiment studies salmon migration in a river and compares split-beam echosounder and video recordings to determine the bias of fish numbers from split-beam fish tracking [Enzenhofer et al., 1998]. They found that split-beam fish tracking in that application was limited by the signal oversaturation when migrating rates were more than 2000 fish/h, thus having a bias of underestimating fish counts through the echo estimates for high echo density [Enzenhofer et al., 1998]. In situations with a high fish density, the split-beam system and fish tracking algorithms are limited by the need to detect and isolate individual fish into single target echoes. However, with the echo integration method, the fish aggregation density can be determined acoustically with enough knowledge of the size distribution of the species or the TS-length relationship [Foote, 1983].

2.3.1 Calibration

The split-beam echosounder is calibrated routinely to have accurate and repeatable measurements. Field calibrations should be performed before and after system deployment. This is done to ensure consistency in measurements of volume backscatter

and to account for any potential drift of values over time due to wear on the the instrument's components. A tungsten carbide calibration sphere is used as a standard target. It is sphere shaped to remove the dependence of target strength on orientation and tungsten carbide is used because of it has well defined acoustic properties [Miyanohana et al., 1993]. The size of the sphere, 33.2 mm, is chosen to avoid resonances that occur in the sphere at the operating frequency of 120 kHz [Foote, 1982]. For the calibration procedure, the calibration sphere is moved in a spiral motion at 5 to 10 m away from the transducer face. The goal is to have about 500 echoes of the calibration sphere per quadrant of the transducer beam. The target strength of the 95th percentile of the targets within -3° and +3° off the center is used to compare with the theoretical value given by the calibration sphere datasheets. The difference between the theoretical target strength value and the target strength calculated in the calibration is used as an offset to adjust the sensitivity drift of the transducer.

2.4 Application to the in-stream tidal industry

The need to monitor fish presence and behaviour in regions of in-stream tidal energy generation motivates the evaluation and validation of fish detection and velocity extraction with ADCPs. High-energy tidal channels are inherently difficult to survey with conventional hull-mounted acoustic instruments. These difficulties affect many aspects of the surveys; in addition to the regular surveying challenges such as vessel noise contamination and weather limitations, the tidal turbulence generated backscatter (bubbles) [Melvin and Cochrane, 2014] attenuates the signal. Sites of tidal energy generation projects are being targeted for the same reasons that make them difficult

to survey, they require high-energy, fast tidal flows. Tidal energy industry converts power from the tidal currents into electricity by installing turbines with blades that rotate similar to wind turbines. Since in-stream turbine technologies do not force migrating fish to pass through dams or enclosures, it is possible that they would have a smaller impact on fish migrations. However, the impact of tidal turbines on fish migratory patterns and stock is not yet understood and requires more research [Shen et al., 2016].

Melvin and Cochrane (2014) set a goal to monitor fish distribution to understand the behaviour (or reaction) of fish when an underwater structure is encountered. They completed nine transects over a full tidal cycle in Minas Passage, a 12 km long and 5 km wide tidal channel, at a location proposed for in-stream tidal power energy conversion devices. Melvin and Cochrane (2014) report that fish in the middle water column are likely to interact with turbines even though the overall density of fish is low, because there is a high density of transient fish in Minas Passage. Melvin and Cochrane (2014) make qualitative recommendations about instrumentation and deployments, such as replacing or complementing conventional boat surveys with stationary or autonomous bottom-mounted echosounders to minimize vessel noise avoidance. Incidentally, these bottom-mounted deployments could lower cost and increase the survey time series length by remaining underwater for several months with minimal boat costs. A long-term assessment of an area could provide the complete dataset required to evaluate the impact of tidal power development on the behaviour and mortality of fish [Melvin and Cochrane, 2014]. Though the recommendations are insightful, they were unable to make quantified conclusions about fish behaviour in

relation to in-stream tidal turbines.

While research on the effect of in-stream tidal turbines on fish behaviour is limited, Viehman et al. (2015), and Viehman and Zydlewski (2017) provide a comprehensive study of the use of the water column by fish and fish abundance in Cobscook Bay, Maine, USA, an area with tidal currents strong enough for tidal power generation. The difficulty of sampling a full tidal cycle in these strong tidal currents conditions had formed a gap in the literature. The research focused on the vertical distribution of fish before the installation of a proposed in-stream tidal turbine to find which populations would be most affected and eventually to compare with vertical densities after the installation [Viehman et al., 2015]. After the removal of the tidal power conversion device, Viehman and Zydlewski (2017) used two years of bottom-mounted moored echosounder data to study temporal variations in fish abundance by completing a wavelet analysis at the location of a removed tidal turbine. Current direction is available for part of the dataset through ADCP measurements, but when this data is unavailable, fish direction is used as an proxy for tidal current, therefore tidal stage. The wavelet transform analysis was successful in finding temporal patterns (modes) in the fish abundance data. However, this study only included individual fish. Fish schools were omitted due to the difficulty in distinguishing them from entrained air and identifying individuals within a school. The importance of continuous long-term sampling in these areas with highly variable fish presence is highlighted [Viehman and Zydlewski, 2017].

ADCPs are essential in any in-stream tidal current analysis due to the need to

measure the highly variable current velocities. These instruments are designed to perform long-term deployments, which is a key factor missing in the literature described above on fish avoidance analysis at tidal energy sites. With the validation of the algorithm proposed by Zedel and Cyr-Racine (2009), fish behaviour studies at various types of research sites could be consistently measured over multiple days, tidal cycles and seasons. In the last five years, there has been some research efforts focused on understanding fish behaviour changes in the presence of tidal turbines. However, research in the field of fish velocity extraction using ADCP instruments does not seem to have kept up, there is a gap in knowledge that could be filled by using the recent tidal energy site research and ADCP's capabilities to extract fish and water velocities.

Chapter 3

Experimental Methodology

To evaluate ADCP performance for fish detection, we designed an experiment that allowed a direct comparison between an ADCP and a split-beam echosounder. This section details the experimental methods. The computational methods are described in Section 4. The experimental methods include the deployment site description, the instruments description, collection settings and calibration as well as an account of the battery power considerations when comparing instruments with widely different battery requirements.

3.1 Experimental Site

The Bay of Fundy is home to some of the largest tides in the world. Grand Passage, Nova Scotia, located on the southeastern side of the Bay of Fundy, has a 5 m tidal range and currents up to 1.5 m/s. Due to these strong tidal currents, it is identified as having the potential for in-stream tidal developments. Prior studies of fish presence in high-energy tidal channels have identified a common survey chal-

lenge to be acoustic scattering from near-surface bubbles [Melvin and Cochrane, 2014, Viehman et al., 2015]. The study by Melvin and Cochrane (2014) recommends deploying "an autonomous, stationary, bottom-mounted echo-sounder" to overcome these challenges. As an experimental site, Grand Passage, NS, further motivates the recommendations because it has frequent boat and ferry traffic. A long-term bottom-deployment allows for inter-survey data which can validate the "snapshot" measurements from conventional surveys. Additionally, diurnal and tidally induced fish behaviour can be separated with a long-term deployment. Acoustic measurements for a comparison of split-beam sonar and ADCP were collected from a bottom-mounted self-contained frame deployed at 25 m depth and positioned as shown in Figures 3.1 and 3.2; note the location was selected to avoid interference from the ferry traffic.

3.2 Deployment

A bottom-mounted frame was equipped with an RD Instruments 600 kHz acoustic Doppler current profiler and a BioSonicsDTX Submersible 120 kHz split-beam echosounder, as shown in Figure 3.3. The 37-day deployment took place from September 21st, 2018 14:30 to October 29th, 2018 13:54. The second deployment was deployed for 28 days from June 11th, 2010, 12:05 to July 9th, 2019, 10:09. The acoustic instruments were installed as close as possible to facilitate direct comparison between both datasets.

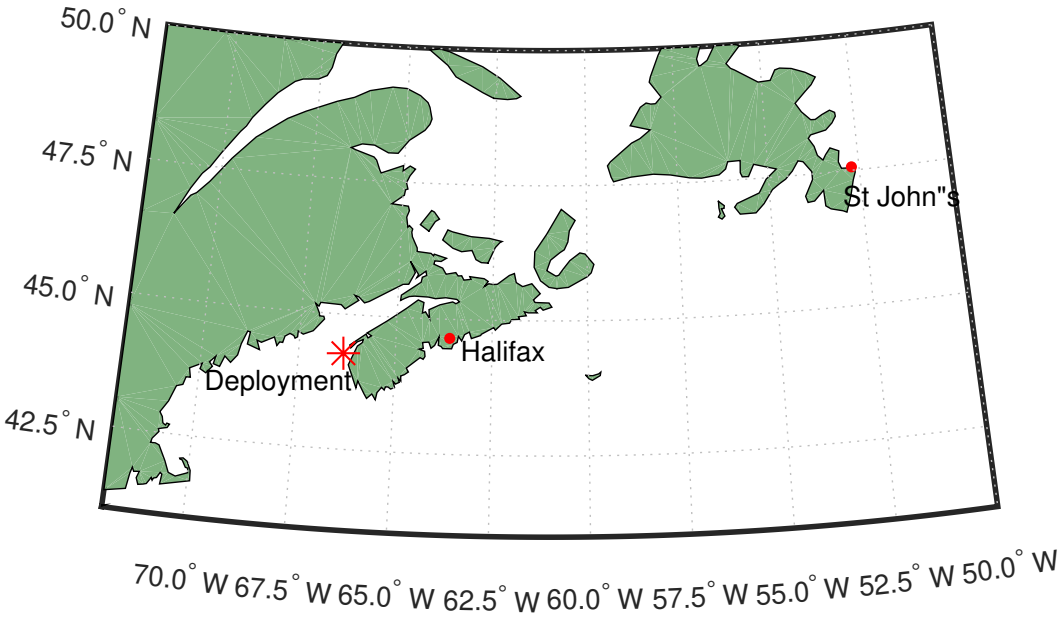

Figure 3.1: Location of the frame in Nova Scotia, Canada.

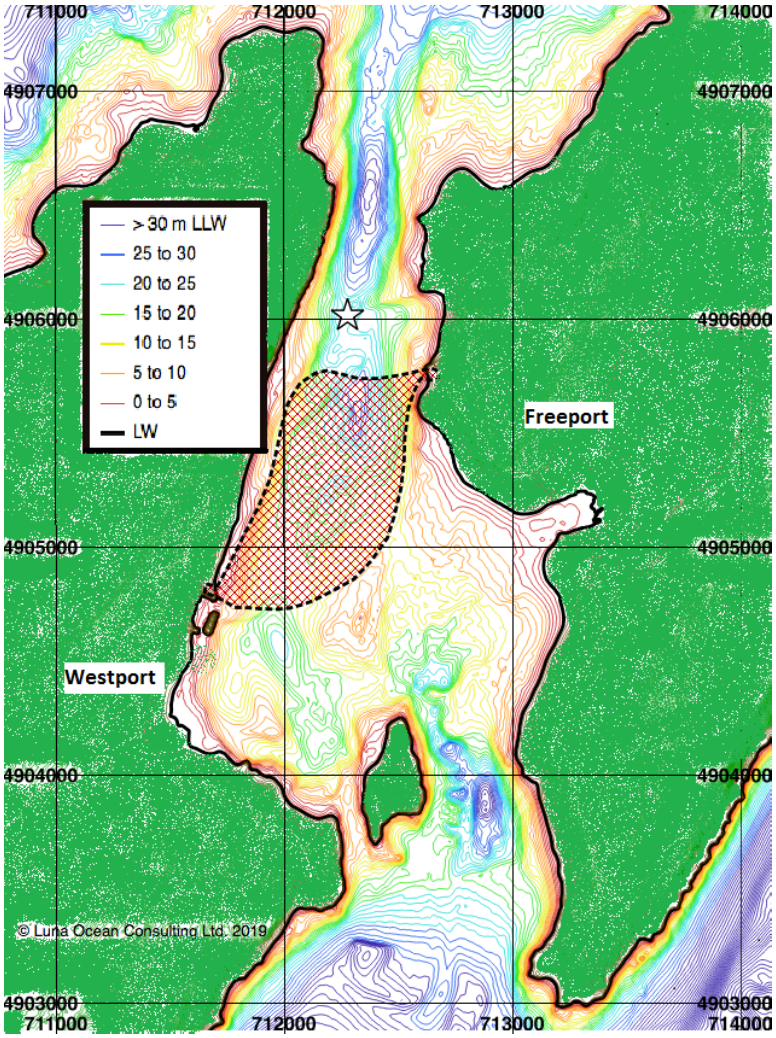

Figure 3.2: Location of the frame ($\star$) in Grand Passage, (extent of the ferry route between *Freeport* and *Westport* is the chequered red area). The green area is land and the isolines are depths at 5 m intervals in the tidal passage, as shown in the legend.

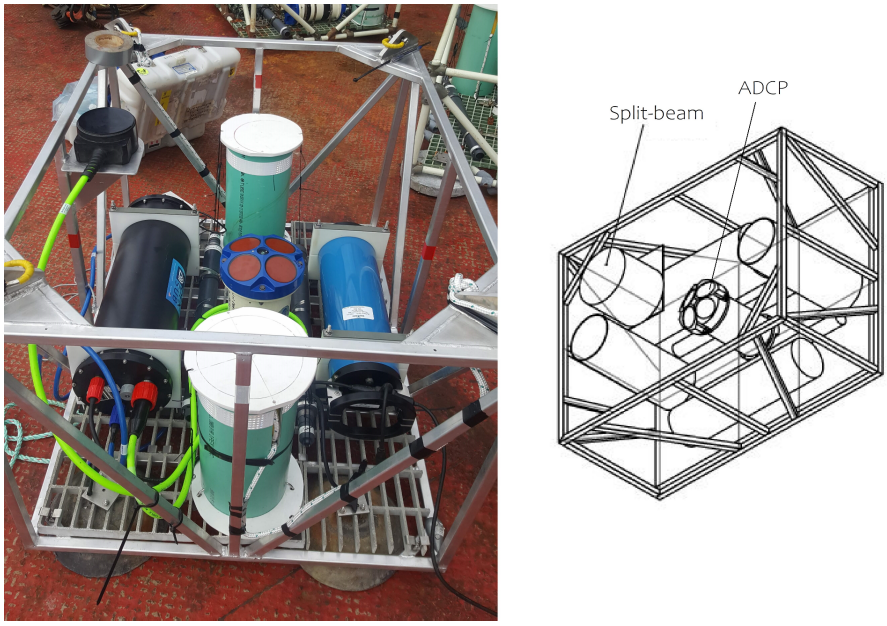

Figure 3.3: Left: A picture of the frame before the deployment with the ADCP in the middle. The split-beam echosounder system includes the echosounder on the shelf, the black horizontal cylinder on the left is the DT-X Submersible and the battery pack is the blue horizontal cylinder on the right. Right: Sketch of the frame designed by Richard Cheel. The frame is 3 by 4 feet.

3.2.1 Duty Cycle

A common problem when operating two nearby acoustic instruments is crosstalk. We chose widely separated frequencies to mitigate this problem (120 kHz for split-beam and 600 kHz for the ADCP). Nevertheless, contamination in the split-beam sonar data was observed during lab tests. Therefore, in addition to the separate frequencies, the duty cycle was staggered to ensure the collection of individual uncontaminated data from both instruments as well as simultaneous measurements. To achieve an offset in the timing of the instruments, the split-beam data acquisition cycle of was started 10 minutes into the ADCP duty cycle.

The ADCP sampling duty cycle was 20 minutes on and 20 minutes off. The Workhorse ADCP time commands from the RDI configuration software were used to set the duty cycle, the chosen settings are summarized in Table 3.1. The time per burst command, TB, determines the length of one whole duty cycle. The ensemble per burst command, TC, dictates the number of ensembles within the burst time. The split-beam sampling regime was 20 minutes on and 40 minutes off.

Upon inspection, the first deployment displayed little contamination between instruments and crosstalk was found to be inconsequential for fish detection. Given that crosstalk did not cause difficulty, the duty cycle was adjusted for the second deployment to maintain the 10 minutes of simultaneous data collection while extending the battery life of the split-beam system. The ADCP was configured to collect data for 30 minutes and be off for 30 minutes while the split-beam was on only for the

middle 10 minutes of the ADCP on cycle.

3.2.2 Data Collection Settings

The ADCP was set to collect at one ping per second with 1 m bins with no averaging of the profile data. It is crucial for the fish detection algorithm that the pings are not averaged. If multiple pings are averaged together the discrete targets, such as fish, will be either averaged out or combined. The time per ensemble, TE, dictates how much time will be averaged in each ensemble and time between pings, TP, sets the ping rate, see Table 3.1 for RDI configuration software commands. Both the time per ensemble and the time between pings must be the same value to have one ping per ensemble, hence no averaging in the time domain. The split-beam sonar was configured to transmit four pings per seconds with a 0.1 ms pulse duration.

3.2.3 Calibration

There are three critical components of the instrumentation that need to be calibrated: the ADCP compass, the ADCP backscatter and split-beam backscatter. The ADCP compass was calibrated the day before both deployments by rotating the mounted frame in a constant magnetic field environment [Instruments, 2001]. The whole frame must be included in the compass calibration to account for any compass offset that may be present due to the magnetic materials of the instrument frame, such as the batteries and any iron material.

Table 3.1: ADCP RDI Workhorse Time and Water Profiling Commands for both the 2018 and 2019 deployments.

Command	Description	Deployment 2018	Deployment 2019
TB	Time per burst	00:40:00.00	01:00:00.00
TC	Ensemble per burst	1200	1800
TE	Time per ensemble	00:00:01.00	00:00:01.00
TP	Time between pings	00:00:01.00	00:00:01.00
WE	Error Velocity (mm/s)	0	5000
WC	Correlation Threshold (counts)	0	0
WN	Depth Cells	30	60
WS	Depth Cell Size (cm)	50	100
WV	Ambiguity Velocity (cm/s)	175	175

The ADCP backscatter calibration coefficients were taken from a January 2018 laboratory calibration. The backscatter calibration was performed following the details described in Section 2.2.2. The split-beam was calibrated using the method described in Section 2.3.1, in the days immediately following the retrieval of the frame. A 33.2 mm diameter tungsten carbide sphere and a 0.4 ms pulse length were used to perform the calibration. The calculated offset of 1.1 dB was applied to the first dataset. The offset from the second deployment was not calculated because the data did not contain fish and was not used for further analysis.

3.3 Battery Considerations

Split-beam echosounders consume significantly more power than ADCPs because they are not designed for long-term autonomous deployments. An accurate battery consumption calculator based on sampling parameters is important for long-term deployments of split-beam echosounders to ensure the collection of enough data over a known period of time. The first step of the deployment design was to calculate the battery consumption of the split-beam system based on collection parameters such as ping rate, pulse duration, duty cycle and range. Initially, the BioSonics DT-X Quick Start Guide [BioSonics, 2016] was used to anticipate the power consumption of the BioSonics Submersible DT-X with one transducer connected. It was quickly established that this would not provide a sufficiently accurate estimate of collection time because it relies on approximations and suggests taking measurements if power draw is of concern.

A series of nine lab tests were performed. Seven tests with unique combinations of data collection parameters as well as a two repeat measurements to develop an algorithm that estimates the battery life. The battery life estimate was based on collection parameters and its variance between repeat measurements. The choice of data collection parameter combinations for the tests was driven by expected deployment need and finding what parameters drove the power consumption.

The algorithm was designed to account for the power draw of the sleep and transmit states and the fraction of time the instrument spends in each state per duty cycle:

$$E_{cycle} = P_{sleep} * \frac{t_{sleep}}{t_{cycle}} + P_{transmit} * \frac{t_{transmit}}{t_{cycle}} \tag{3.1}$$

where P is the power draw for the *sleep* or *transmit* state, t is the amount of time spent in the *sleep* or *transmit* state, determined by the duty cycle and E_{cycle} is the energy used for one full cycle.

The total operating life was then calculated from the ratio of the total energy available and the energy used for one cycle.

$$t_{total} = \frac{E_{available}}{E_{cycle}} \tag{3.2}$$

where $E_{available}$ is the total amount of energy available (Wh) in the battery pack.

In determining the values for the power consumption terms in Equation 3.2, the goodness of fit was evaluated using the percentage difference between the the lab tests and the calculated operating life. The test initial results, taken with a profiling range of 100 m, were within 2% of the observed total sampling time. When the profiling range was set to 30 m, which was the case for the deployment, the difference between Equation 3.2 and the observed duration was 30%. This unexpected result had shown that a shorter profiling range uses more power. To account for this increased power draw, Equation 3.2 was modified with an adjustment term that accounts for changes in operating range:

$$t_{total} = \frac{E_{available}}{E_{cycle}} - \frac{(100 - R)}{10} \tag{3.3}$$

where R is range in meters. With the additional term, an average of 7% error was achieved.

The standard battery pack for the BioSonics Submersible system is a DeepSea Power & Light rechargable battery, rated at 960 Wh, but that system didn't provide the total power required for the deployment we had planned. We instead selected an OceanSonics Subsea battery pack that provides 4500 Wh with lithium primary batteries. We used the battery consumption function to select a set of parameters (ping rate at 4 pps, pulse length at 0.1 ms, duty cycle set to 20 mins on and 40 mins off and a range of 30 m) that would provide a 24 $\pm$ 3 days of operating life given the power available (see line 1 of Table 3.2). However, only 8.6 days of data collection was realized. The discrepancy in collections days was partially explained

by the strain of high current draw (200 mA) on the lithium-ion primary D-cells which caused them to derate significantly. Discharge curves in the technical data sheet were used to quantify the derating of each battery cell due to the high current draw [SAFT, 2010]. Using the corrected available power, 2500 Wh rather than 4500 Wh, the battery consumption function determined the battery pack should have had 14 $\pm$ 1 days of operating life, which was closer but did not account for all the missing days (see line 2 of Table 3.2).

While preparing for the second deployment, a short on the circuit board was found to have been causing an additional constant power draw of 100mA, limited only by the current limiting components in the battery pack. However, this short still reduced the effective power capacity of the battery, which accounts for the additional missing days of data collection (see line 3 of Table 3.2). The second deployment was designed with a duty cycle of 10 minutes on per hour rather than 20 minutes on per hour to increase the expected collection time to 26 $\pm$ 3 days (see line 4 of Table 3.2). The second deployment yielded 24 days of data collection, which is within the expected value and demonstrates the utility in the battery consumption function (Equation 3.3).

Table 3.2: Total collection time calculated by the battery consumption algorithm based on different collection parameters and available power. Nominal is the ideal conditions ratings (3.6V, 17Ah). Derated is the rating estimated +10°C with 200mA current draw (3.2V, 11Ah).

72 Lithium Batteries	Voltage	Energy	Collection	Error
Nominal	21.6 V	4406 Wh	24 days	± 3 days
Derated	19.2 V	2534 Wh	14 days	± 2 days
Derated + Short in Circuit	19.2 V	2534 Wh	9 days	± 1 day
Derated + New Duty Cycle	19.2 V	2534 Wh	26 days	± 3 days

Chapter 4

Computational Methodology

This chapter on computational methodology provides an overview of BAMFF, the suite of custom MATLAB scripts used to batch process the ADCP data for fish detections. Sonar5-Pro, the software used for post-processing and fish tracking the split-beam echosounder data is described. Also, we outline how fish are identified and isolated with the use of thresholds for both systems.

4.1 Broadband Acoustic Monitoring For Fish (BAMFF)

The Broadband Acoustic Monitoring For Fish (BAMFF) package was used to process the ADCP data. It is a MATLAB toolbox that processes raw ADCP data into depth and time-averaged fish and water velocities. The toolbox converts the RDI files into user-modifiable MATLAB structures, then it calibrates and corrects for spherical spreading and absorption loss using the procedure outlined by Deines (1999) [Mullison, 2017]. Using the combination of correlation and volume backscatter thresholds, it determines whether signals are from fish or water targets in each beam

individually. The targets for all the beams are sorted by time and depth to calculate the average fish velocity and count. It also bins the non-fish target in the same way to extract the water velocity profiles.

4.1.1 Thresholds

As with any echosounder system, the presence of fish in the Doppler sonar data can be initially assessed by volume backscatter levels exceeding a specified threshold. In addition, properties unique to the broadband Doppler system allow discrimination of discrete targets as opposed to volume backscatter. The correlation processing inherent to broadband sonar provides an alternative way to detect discrete targets. In contrast to correlation coefficient values of 0.5 or 128 counts, a characteristic expected from a cloud of bubbles, more extensive school of fish or an absence of discrete targets, discrete targets create peaks in the autocorrelation. A perfect single discrete target without noise would return a correlation value of 1 or 256 counts, as recorded by the RDI systems [Tollefsen and Zedel, 2003]. The correlation threshold aims to isolate the high peaks in the autocorrelation signal that is indicative of a discrete target, such as a single fish target when it coincides with high volume backscatter signal.

The threshold values were determined by starting with low values and slowly increasing them while assessing their accuracy on a characteristic single fish school and a bubble plume. The thresholds were increased until the bubbles plume was not considered to include discrete targets, but the fish in the aggregation were still detected. The balance between the intensity and correlation thresholds was adjusted further so

that in general other bubble plumes and fish schools were correctly identified.

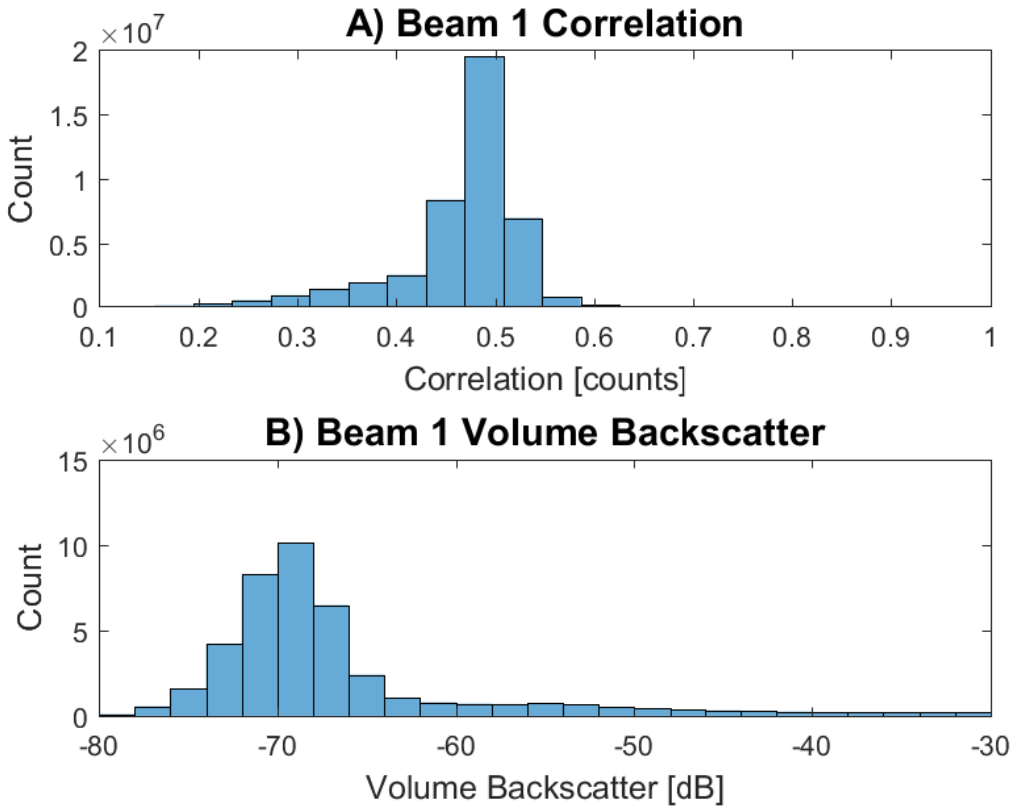

Figure 4.1: Histograms of the a) correlation and b) volume backscatter values in beam 1 for the 2018 deployment.

Figure 4.1a shows the correlation has a sharp upper limit where no targets are detected with a threshold above 159 counts (or 0.62). For the second deployment, this limit increases to 190 counts because of the decreased size of the depth bins. The smaller depth bins, 0.5 m for the second deployment compared to 1 m for the first,

increase the likelihood of a target to be discrete within its bin because it is averaged over a smaller sample volume. The intensity counts sharply decrease and taper off at volume backscatter values above -65 dB (Figure 4.1b).

The volume backscatter and correlation thresholds are applied to each beam individually for fish detection. An example of the effect of the thresholding is shown in Figure 4.2. The top left panel, Figure 4.2a is the sonogram image based on the calibrated volume backscatter, S_v from beam 1. Figure 4.2b is the calibrated volume backscatter, S_v, with a threshold of -45 dB applied to isolate all possible fish target candidates. It results in bubbles, surface and fish targets remaining. The correlation threshold of 153 counts (or 0.60) is applied to finalize the fish detection by removing the low quality, incoherent targets. In addition to the thresholds, the near-field and the surface must be removed from the analysis.

The near-field is the area of non-uniform phase structure at the face of the transducer. Near the transducer face, the signal is complex because it has areas of constructive and destructive interference [Medwin and Clay, 1997]. Past a critical range, determined as $R = \pi \frac{a^2}{\lambda}$, the pressure is safely far-field and the phase is uniform across the beam. With a transducer radius, a, of 0.04 m and a wavelength, λ, of 0.0025 m, the near-field range is calculated to be 2.0 m. Only the far-field signal was kept by excluding first 2 m from the analysis. As for the surface, the exclusion line range was selected with a running mean of the maximum volume backscatter. This exclusion line removes the strong surface backscatter and anything beyond the surface from the analysis. The final targets remaining after the volume backscatter threshold, the cor-

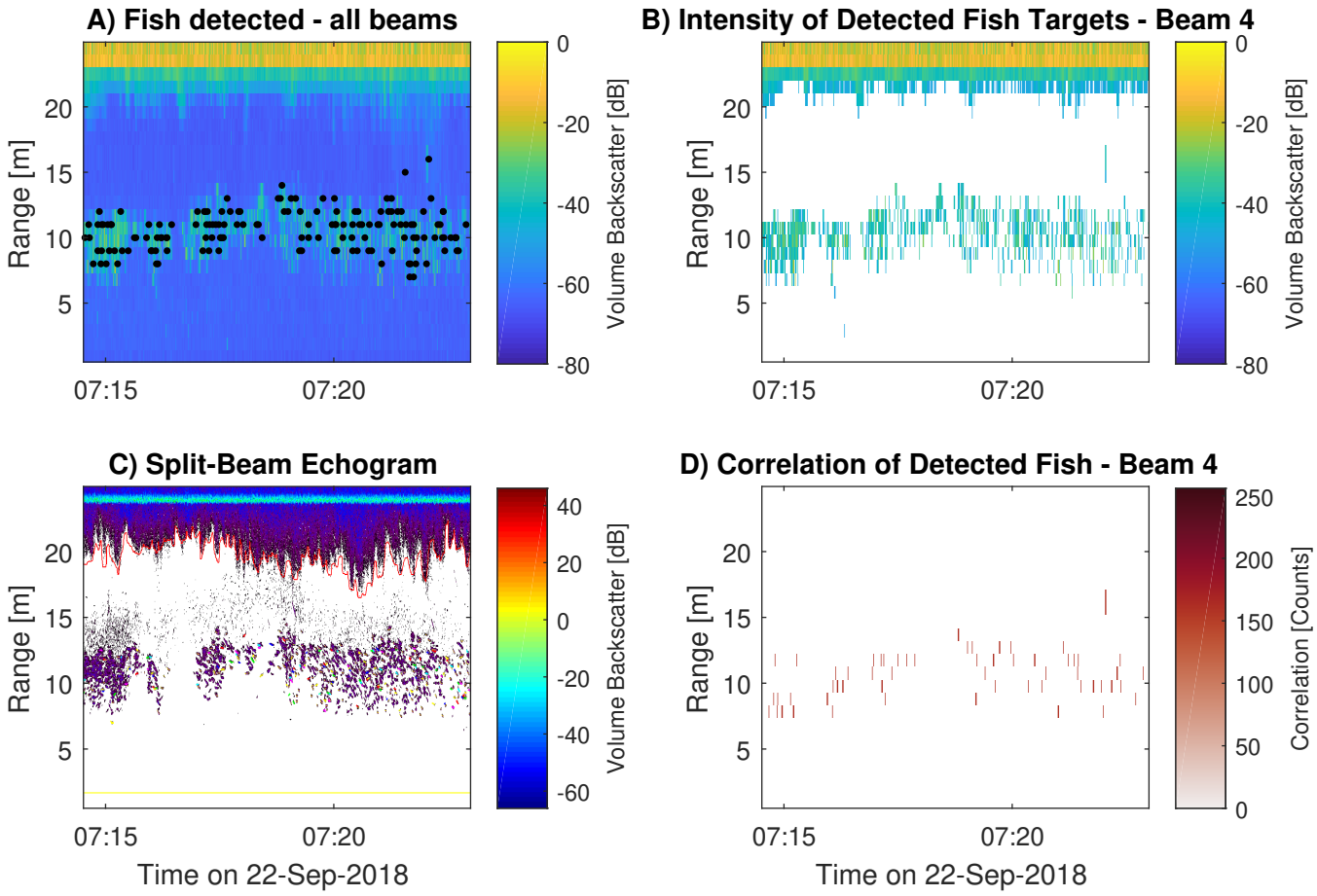

Figure 4.2: a) A volume backscatter sonogram for a fish school from the ADCP with the identified fish targets (black dots, ·) from all four beams b) identifies the remaining data after the backscatter threshold (-45 dB) is applied, c) the corresponding split-beam signal and d) identifies the remaining data after the backscatter and correlation thresholds (135 counts).

relation threshold, and the surface and near-field exclusion lines are accepted as fish target; these are shown in Figure 4.2d and as well, these remaining detected targets are indicated by black dots in Figure 4.2a. Note in particular the clear agreement in backscatter structure when comparing the Doppler sonar data (Fig. 4.2a) with the split-beam data (Fig. 4.2c). Conversely; water targets are identified as signals below either the intensity or correlation thresholds; and these water target data are used to calculate the water velocity.

4.1.2 Refactoring

To make the BAMFF toolbox more accessible to potential users, some tactical refactoring was undertaken to make the code run easily for any data collection parameters and surveying or deployment configurations. Tactical refactoring with regards to programming means to improve and redesign existing code with an end goal that is beyond the requirements of a current task. The goal of the present refactoring was to make fish detection, and velocity extraction as well as water velocity extraction easily accessible for a user with a raw ADCP data file through this suite of functions. The refactoring started with renaming functions from their corresponding name in the RDI software package to descriptions of what is accomplished by running the function. Naming the functions based on their task removed the dependence of having to understand the RDI software package to use this package. For example, the code component that converts RDI raw data into variables in the MATLAB environment is called RDItoMAT.m.

Because ADCP processing is often associated with large datasets, the focus was then put towards reducing the amount of coded loops in the software. The loops were replaced with logical indexing when possible to increase speed and the readability of the code. The speed of the code was also improved by reducing the amount of times data files were opened and closed because this file activity takes up the most amount of time in this package. The code documentation was reviewed; comments that helped follow the code when the purpose of certain lines might not be obvious were kept to improve readability. Comments regarding debugging checkpoints and questions were addressed and removed. During the refactoring, a structure containing all of the parameters that can be saved with the raw data was formalized as a function. This parameter structure maintains a summary of the collection and post-processing parameters used for the survey and the analysis. The structure format facilitates switching between datasets with different post-processing requirements and instruments with different calibration coefficients. Aditionally it allows the user to revisit the analysis if the need arises.

Visualizations tools are the clear next step required in the package. However, optimal data visualizations vary depending on the purpose of the post-processing.

4.1.3 Documentation

The BAMFF code is published in a repository and is maintained under version control. Documentation for the toolbox is on a Read the Docs webpage, www.bamff.readthedocs.io. The landing page of the documentation webpage is included in Appendix A. The web-

page includes a description of the package and a Literature Review for background information that might be required by a user. The algorithm documentation section describes all the entries in the parameters structure with some suggested values for starting off. It also contains a brief summary of the main functions required to get from raw RDI data files to fish targets. There is also a Quick Start guide that provides a generic run-through of the package. Lastly, reference are provided for additional information and in case the package should be referenced for another project.

4.2 Split-beam with Sonar5-Pro

Sonar5-Pro [Balk and Lindem, 2017], is a sonar post-processing program developed to improve single echo detection methods for fish target detection in sonar data. Balk and Lindem (2002) created a split-beam sonar target tracking algorithm to improve "traditional" methods that would frequently miss echoes from fish and create tracks solely from noise. This program, like many others of its kind, requires the user to establish the zones that will not be evaluated for fish detection, such as the near-field and the surface or bottom. Double the near-field range is commonly used for the exclusion zone in front of the transducer, for the Biosonics 120kHz split-beam echosounder the near-field is 0.73 m; the exclusion zone is set to 1.46 m. In our case, the ocean surface also needs to be excluded by a surface exclusion line. This problem is analogous to difficulties near the bottom for conventional hull-mounted (downward looking) system operations. In the present application it is possible to use the bottom detection algorithm to identify the location of the surface. Generally, the bottom

detection algorithm requires manual adjustment when fish are near the surface and when the fish and bubbles are mixed. For this purpose, the software provides facility to adjust the exclusion lines. The manual adjustment process is a visual judgment of the sonogram image to delineate the extent of the spreading bubble plume. Manual adjustments can introduce bias by either keeping too much of the bubble plume which results in false targets from bubbles or by eliminating too much which leads to an inaccurate fish count estimate. In addition, it is time-consuming for the user and results in blind spots for the system.

The Cross-Filter Detector algorithm, developed by Balk and Lindem (2002), was used to identify the SED and to combine them into fish tracks. There are four components to the Cross-filter Detector for tracking: the detector, the evaluator, the SED and the tracking. The parameters for each component were tuned by carefully following the guidelines described in the Sonar5-Pro manual [Balk and Lindem, 2017]. The same fish school used for tuning the ADCP parameters was used to choose the settings for fish detection and tracking.

The first component of the Cross-Filter Detector algorithm, the detector, is composed of two filters: a foreground filter that smooths over the stronger signal with a running mean and a background filter that averages over the ping-to-ping intensity fluctuations without modifying the echoes from fish. The background filter is a key component in the algorithm as it suppresses the noise that causes missing fish targets and false noise targets. The combination of the foreground and background filters creates an adaptive threshold used to isolate the fish targets from the rest of the

signal [Balk and Lindem, 2002]. The filter values were changed until the background filter removed the background noise and the foreground filter made the targets in the fish school stand out without causing the targets to overlap.

When the Cross-Filter Detector foreground and background filters have been completed, the evaluator is used to remove unwanted detections by considering the image and fish tracks as a whole. The fish school was used to make a training set for the evaluator parameters by identifying targets that are wanted. Only one setting was turned on at a time, the auto-detect option provided by Sonar5-Pro was used to provide estimates of appropriate values for each setting. Using the most effective settings from the the auto-detect testing, the criteria that worked best for removing unwanted detections in the present dataset were the track length, mean intensity and standard deviation parameters, as shown in Table 4.1.

The SED component of the Cross-Filter Detector algorithm produces a SED echogram without missing detections and without noise detections. The echo separation parameter was used to determine the maximum allowed gap in time between detections, determined in pulse lengths. It was determined to be 3 pulse lengths based on visual inspection of the SED results.

In the tracking component of the Cross-Filter Detector algorithm, the SEDs identified in the previous step are combined into fish tracks using a simple multiple target tracker (MTT) algorithm. The simple MTT is based on a proximity threshold, which is determined by the gating parameter, set in meters. The gating parameter defines

a conceptual gate that is formed around a track and determines if a single observation is within the gate of the track and not within the gate of any other track [Blackman, 1986]. The tracks are accepted or rejected depending on length, speed and path which are determined based on the site, species and data quality. The track parameters used are reported in Table 4.1, they were determined by visual inspection of the detected fish tracks in the sonogram of the characteristic fish school.

The parameters of the Cross-Filter Detector for tracking chosen for the first deployment were expected to be adequate for the second deployment. However, only 110 fish were detected when using these setting over the 24 days of the second deployment. The detector filters were modified to favour the possible fish targets, and many settings had to be turned off in the evaluator to keep as many detections as possible as reported in the deployment 2019 column of Table 4.1. The need to reduce the parameters to accept almost anything to detect a few fish, suggests that the dataset has too few fish targets to determine settings appropriately. False targets were being accepted in order to detect fish targets within the few small schools that were present. As a result of this low rate of fish occurences, no comparisons between ADCP and split-beam were possible for data from the second deployment.

Table 4.1: Parameters for each component of Cross-Filter Detector for tracking algorithm Sonar5-Pro.

Component	Parameter		Deployment 2018	Deployment 2019
Detector	Foreground Filter	Height	15 bins	17 bins
		Width	5 pings	7 pings
	Background Filter	Method	Mean filter	Mean filter
		Height	53 bins	39 bins
		Width	5 pings	5 pings
		Offset	10 dB	10dB
Evatuator	Track Length	Min.	4 pings	/
		Max.	32 pings	/
	Mean Intensity	Min	-50 dB	-70dB
		Max	-28 dB	-28dB
	Std. dev. Alo	Min.	0.97	/
		Max.	5.87	/
	Std. dev. Ath	Min.	0.51	/
		Max.	6.73	/
SED	Max gap between detections		3 pings	3 pings
	Range detection		Center of gravity	Center of gravity
Tracking	Min. Track Length		5 pings	2 pings
	Max. Ping Gap		2 pings	5 pings
	Gating Range		0.05 m	0.02 m

Chapter 5

Results

A total of 37 hours of simultaneous data were collected in 10 minute intervals during the first deployment between September 21st and November 1st, 2018. The second deployment did not qualify for further analysis because it does not have enough fish detections in either instrument, less than 110 fish counts in the split-beam over the 90 h of simultaneous data. Results from the first deployment show that the detected fish targets of the ADCP and split-beam datasets generally coincide in time and space. The ADCP has a slightly lower count in the dense fish schools but seems to detect more isolated targets.

5.1 Fish detection

The accepted fish detections for both instruments were averaged over 2 h time bins and 2 m depth bins. The temporal bin size was chosen to have enough data points to average (20 minutes of data in 2 hours) without averaging over tidal cycles. The

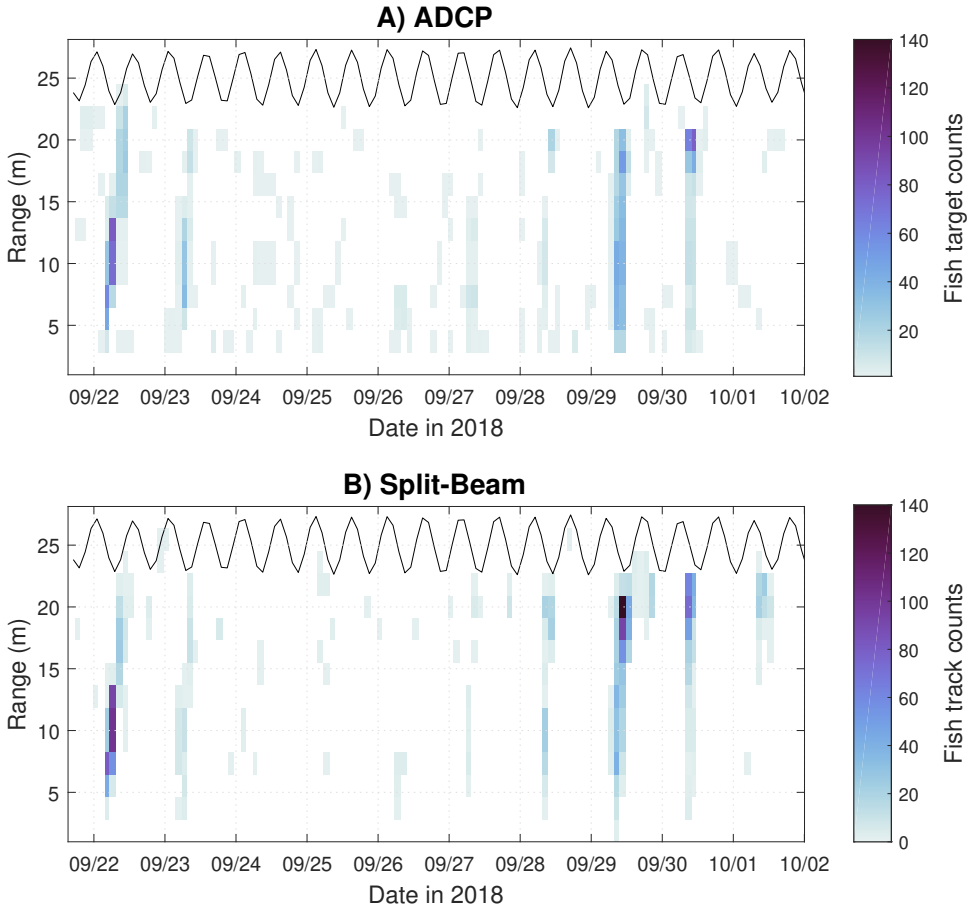

Figure 5.1: Fish counts of the simultaneous data collected averaged over 2 h time bins and 2 m depth bins. a) ADCP fish targets, b) split-beam fish track count.

2 m depth bins were chosen to have two bins to average in the ADCP data while maintaining the depth structure of the fish aggregations. Smaller depth bins fragmented the results. The resulting data summarized in Figure 5.1 shows an agreement in the intervals of higher fish detections. The split-beam generally has a couple of bins with a higher density of fish than the ADCP within each fish school. The more dense areas in the split-beam fish school detections are most noticeable with the fish schools on September 22nd and September 29th, 2018. However, fish counts for both instruments are similar in other aggregations and span the same depth range.

The fish detections from Figure 5.1 were depth-integrated (Figure 5.2a). The peaks, representing the fish schools, occur at the same time in both the ADCP and split-beam. Notable differences in between the datasets (Figure 5.1b) are seen in the fish schools on September 22nd and 23rd, which show a greater number of ADCP fish detections, and the fish school on September 29th and 30th, and October 1st, 2018, where more split-beam fish targets are detected. Both of these occurrences are relatively small schools with less than 100 fish detections.

The depth-integrated time series was also analyzed with the fish counts on a logarithmic scale to asses any differences within periods with much lower fish detections, Figure 5.3. Figure 5.3 shows in general good agreement between ADCP and split-beam observations across all fish concentration values.

The data of the depth-integrated time series (Figure 5.3) were used to calculate the linear regression between split-beam SED and fish tracks with ADCP fish counts.

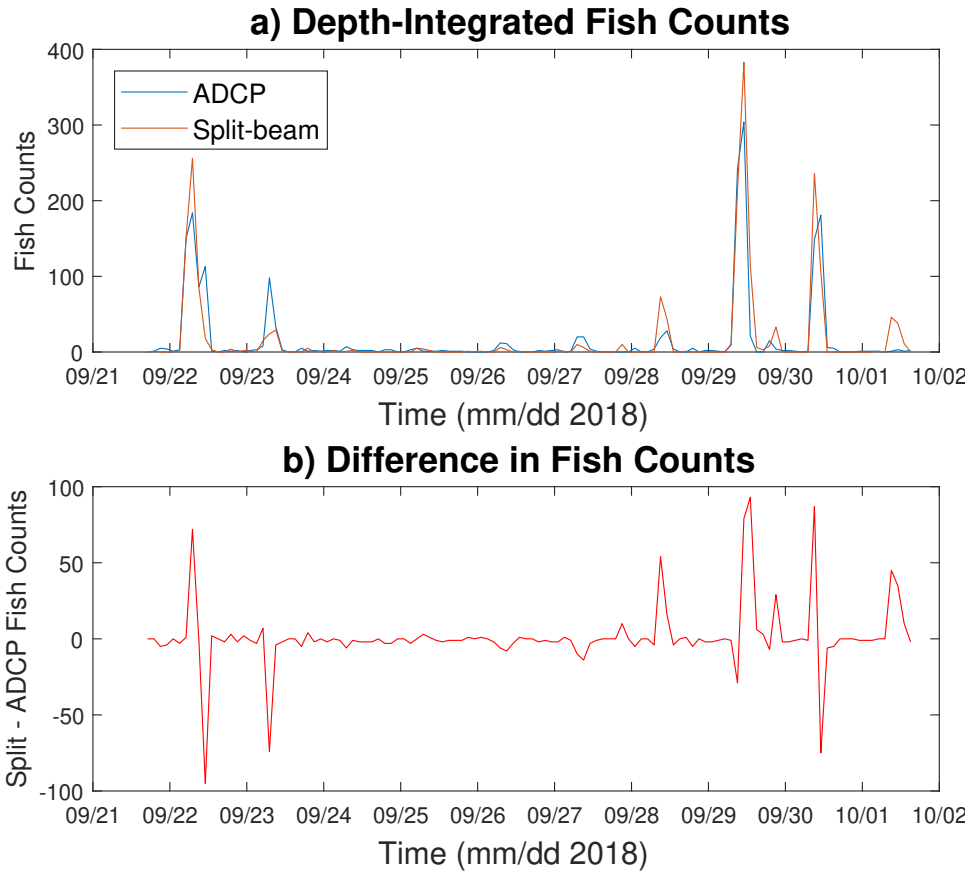

Figure 5.2: Fish counts of the simultaneous data collected depth-integrated and averaged over 2 h time bins. a) The ADCP fish targets counts are plotted in blue and the split-beam fish tracks are plotted in orange. b) The difference between the split-beam and ADCP fish counts, positive values is when there is more fish counts in split-beam, negative values when there is more ADCP fish count.

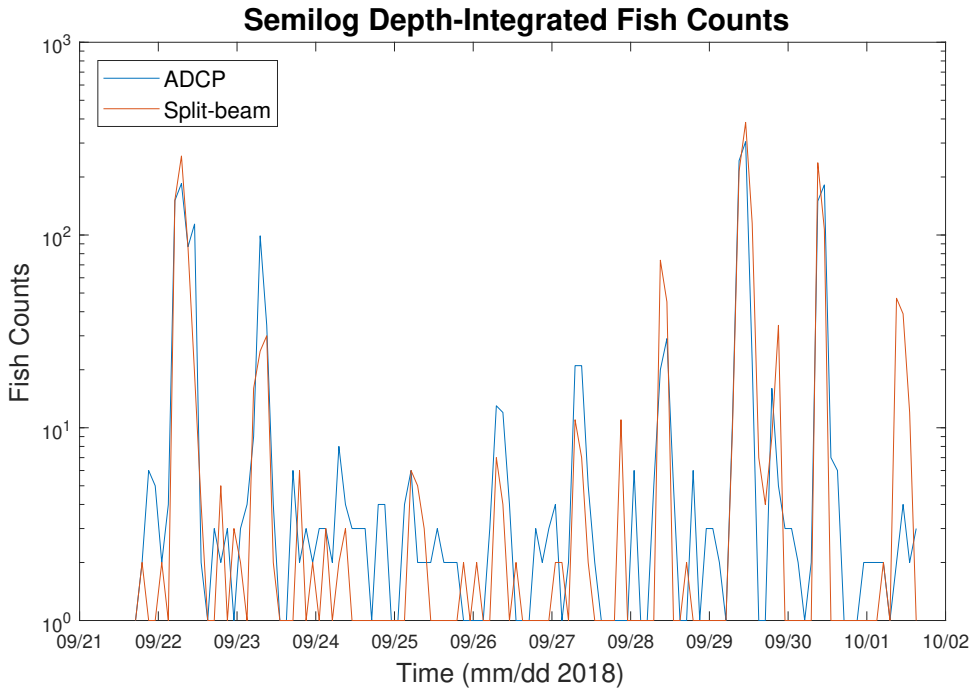

Figure 5.3: Fish counts of the simultaneous data collected depth-integrated and averaged over 2 h time bins on a semi-logarithmic plot. The ADCP fish targets counts are plotted in blue and the split-beam fish tracks are plotted in orange. The values with zero fish were set to 1 to accommodate the semi-logarithmic plot.

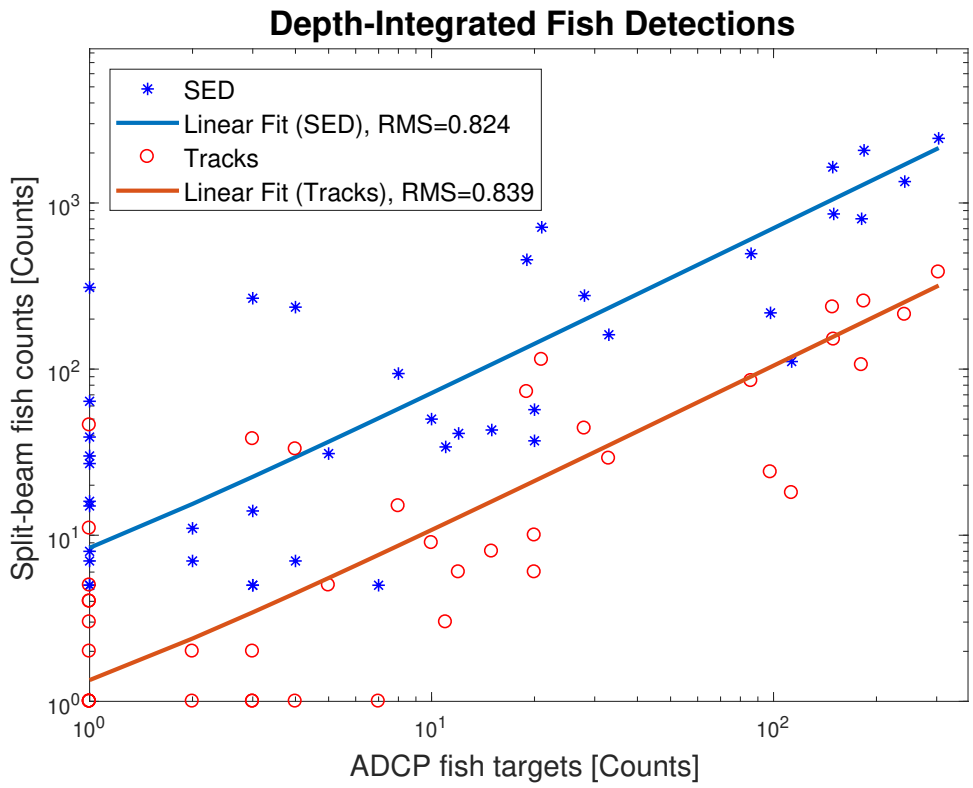

Figure 5.4: Linear regression analysis for comparison of overlapping ADCP fish targets dataset to split-beam fish track counts and SED within fish tracks count, both datasets were averaged in 2 h time bins and depth-integrated for the whole water column.

Although analysis was carried out using observed values, a scatter plot (ADCP vs. split-beam) is presented using a log-log plot in Figure 5.4 in order to highlight agreement at both high and low fish concentrations. When compared against the fish targets identified by the ADCP, a slope of 1.04 ± 0.3 for the fish tracks and 7.0 ± 0.3 for the SED of the split-beam was calculated for the linear regression. The SED comparison indicates that there are on average seven single echo detections per ADCP fish target. Overall, a cross-correlation coefficient of 0.92 was calculated between the fish tracks from the split-beam and the fish counts from the ADCP. The p-value for both dataset comparisons are on the order of 10^{-40}. The y-intercept exists in the SED linear regression (Figure 5.4) because in log space, the y-intercept, b, (at x=1) reflects the slope from the linear domain ($b = log_{10}m$).

It is important to note that the track and ADCP detection agreement seen here is rather circumstantial. The detection volume and sampling rate are different between the two systems. In this case it is just that the system sensitivities for the targets being counted have by chance scaled the actual count values to agree quite closely. More generally, what is important is the linear relationship between the two counts.

5.2 Target strength

There are a number of reasons why agreement of target strength values between the two instruments would not be expected to agree, most critically, the frequency difference and the absence of a precision calibration for the ADCP. However, the results were compared for the shape of distribution. The volume backscatter strength was

calculated using Equations 2.5 and 2.6. The resulting target strength values show a bimodal distribution for the ADCP data (Figure 5.5) which could suggest that the isolated fish targets were from two different taxa, likely fish and zooplankton. In contrast, the TS distribution of the split-beam shows only a unimodal distribution at slightly greater values.

The data from Figure 5.1 was converted to average target strength (Figure 5.6) in order to asses any spatial structure in target strength values. The ADCP binned TS detections (orange histogram in Figure 5.5) show the lower TS range, from -70 to -60 dB re 1 m^{-1}, corresponding to the isolated detections in Figure 5.6a where the split-beam did not have any fish detection. Comparing with the fish count time series, Figure 5.1, it is evident that the greater target strengths are from dense aggregations. At the same time, the isolated targets identified by the ADCP correspond to the weaker peak (-70 to -60 dB re 1 m^{-1}). The difference in frequencies could account for the detected targets with smaller echoes present in the ADCP (600 kHz) histogram that were not in the split-beam (120 kHz) histogram. The 120 kHz instrument would be unable to measure as small of targets as an 600 kHz instrument because greater frequencies can detect targets that are smaller in size. The split-beam is the industry standard for target strength measurements because it removes the effect of the beam pattern from the backscattered signal. The ADCP data from its four single beam transducers are convolved with their beam pattern because the target can not be located within its beam. Also, the ADCP beams are slanted at a 20° angle unlike the split-beam where the beam is oriented vertically. The directivity contributed to the spread in the TS distribution of the ADCP because of the dependence of the

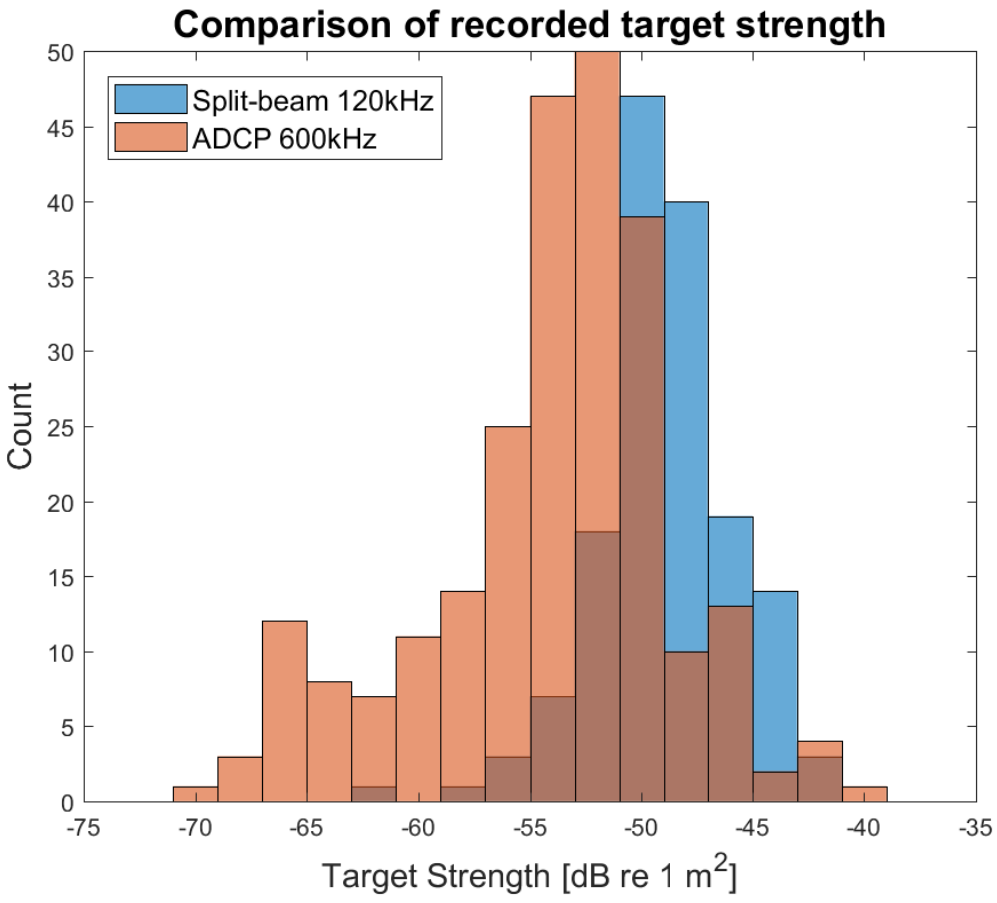

Figure 5.5: Histogram of target strengths observed with both instruments, averaged over two hours and 2 m depth bins. The orange bars are ADCP, the blue bars are split-beam and the third colour is the overlap between the two instruments.

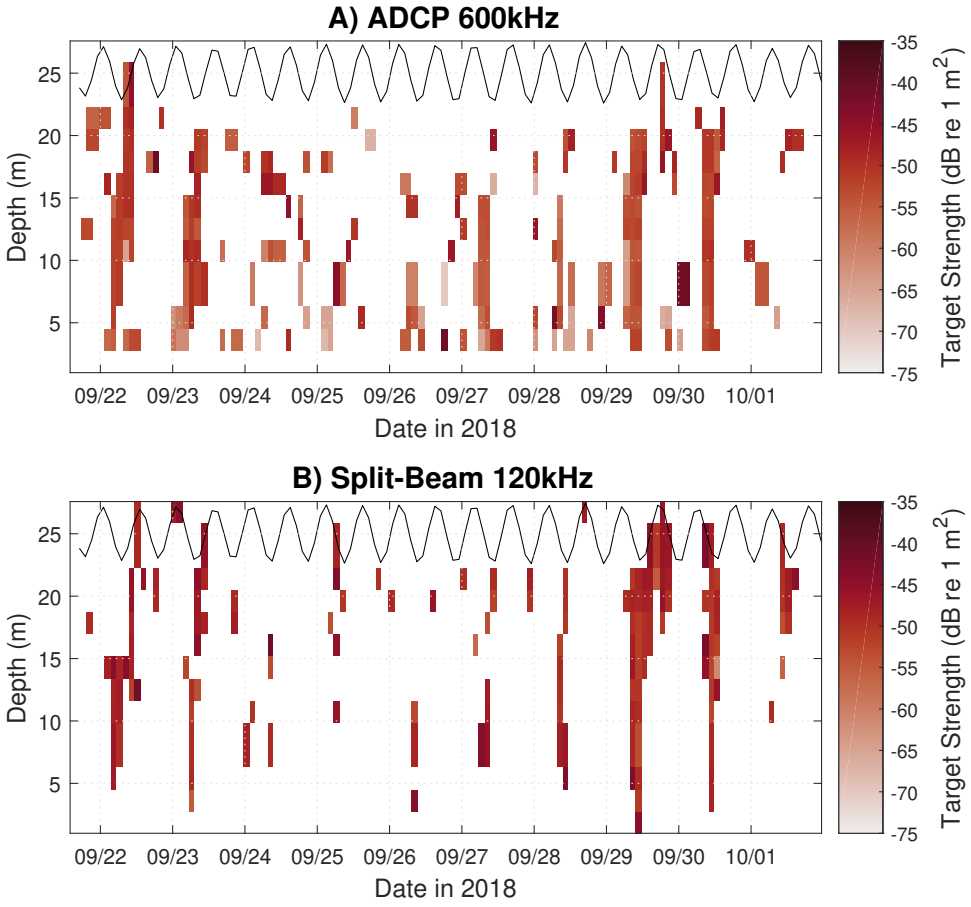

Figure 5.6: Fish counts for the simultaneous data collected averaged over 2h time bins and 1m depth bins. a) is the ADCP fish targets and b) is the split-beam fish track count.

backscattering cross-section on the tilt angle of the fish [Foote, 1983].

5.3 Entrained air

A particular challenge in strong tidal flows is the occurrence of near-surface bubble plumes [Melvin and Cochrane, 2014] which are often hard to distinguish from fish (or plankton) targets. By using a bottom-mounted frame rather than a hull-mounted survey, the data in the present study extends right up to the surface. The zone just below the surface must be clear of entrained air to be analyzed with the split-beam echosounder, because the bubbles are notorious for false detections with fish detection and tracking methods.

The surface exclusion line, red line in Figure 5.7a, determined the upper limit for the analysis area and had to be adjusted manually for this area because bubbles and fish are mixed together in the sonogram. Arguably the whole zone above 15 m depth should have been removed from the analysis, but inspection of the echosounder image suggested clear fish targets within the bubble plumes. For the data shown in Figure 5.7b, the Doppler sonar volume backscatter shows the fish targets identified below and within the bubbles. The requirement of coincident high signal correlations and high intensity was used to distinguish discrete targets from bubble clouds. In this case, the ability of the ADCP to differentiate between bubbles and through the use of the correlation values fish target is a promising result that demonstrated that ADCP fish detections could complement traditional survey methods in areas of high

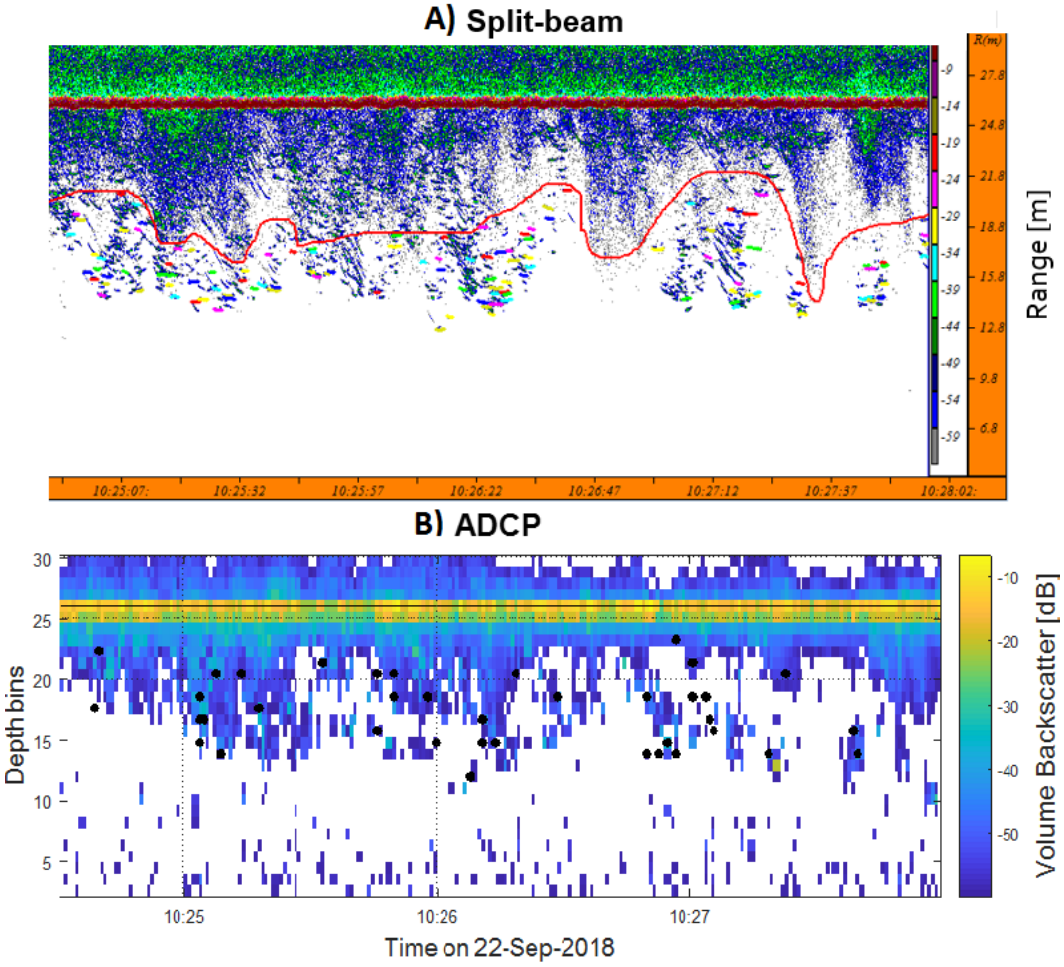

Figure 5.7: Fish detections in entrained air: a) shows the split-beam fish tracks (colorful lines) below the surface exclusion line (red curvy line) and b) shows ADCP fish detections intermingled with the bubbles. The surface is at 25 m: a) the dark red horizontal line, b) the orange horizontal line.

turbulence.

Chapter 6

Discussion and Future Work

6.1 Discussion

This thesis presented the acoustic data and results of a comparison between a broadband ADCP and a split-beam echosounder from a 37-day deployment in a high-energy tidal channel. This research assessed the ability of a broadband ADCP to detect fish. Depth-averaged fish targets from the collocated instruments show a strong agreement for the 370 minutes of simultaneous data. This result demonstrates that broadband ADCP results agrees with split-beam echosounder results for fish detection. The agreement of the datasets suggests ADCPs can be a promising alternative fish detection method.

Single fish detection and target tracking is difficult in fish schools for split-beam sonars. When aggregations are too dense, fish cannot be individually isolated and their tracks, or velocities, cannot be extracted. The ADCP detected fewer fish in

denser areas of fish schools. The bin size difference, 1 m for ADCP and 0.15 m for split-beam is suspected to contribute to the discrepancy. With a smaller depth bin size the broadband ADCP should be capable of detecting discrete targets in denser areas. By simply relying on the combination of high correlation and high intensity values, the ADCP avoids the target tracking challenges that come with high concentrations of fish. However, even with a smaller bin size, the ADCP would also under represents the fish counts in dense aggregations.

Bubble plumes caused by entrained air were excluded from analysis in split-beam data to reduce the number of false detections. For single echo detections and target tracking, a fish cannot consistently be distinguished from a bubble plume. With the correlation threshold, the ADCP was capable of detecting fish in zones with entrained air by differentiating bubbles clouds from fish targets, as shown in Figure 5.7. The added capabilities of the ADCP showed it isolated fish targets in areas unaccessible for fish detection to the split-beam. However, this comparison is biased due the effect of the difference in frequencies on the backscattered signal of bubble plumes because higher frequencies are less affected by bubble clouds.

Comparisons between the presented ADCP and split-beam data are also complicated by discrepancies in the collection parameters, more specifically, sample volume and ping rate. With a 25 m range, the split-beam has a sample volume of 0.47 m^3, whereas the ADCP's sample volume is 0.76 m^3, when including all 4 beams. Consequently, the ADCP measures over 1.5 times the volume of water for each ping. Considering the ping rates discrepancy, the four pings per second ping rate of the

split-beam echosounder could make up for the sample volume difference relatively to the one ping per second rate of the ADCP. The ping rate for the split-beam must be higher to detect each fish target at least twice for fish tracking, a requirement established in the Sonar5-Pro tracking parameters. The ADCP only detects each fish once because of the single detection framework of the ADCP target detection method. However, for flow rates greater than 0.7 m/s, the ADCP could miss fish detections at 25 m range from the instrument that the split-beam would be able to detect twice and successfully track.

These results answer our guiding questions:

1. Can ADCP accurately detect fish? The fish detectability data demonstrates that broadband ADCPs can detect fish in providing agreement with the industry standard, split-beam echosounder, for the conditions sampled in Grand Passage, NS.

2. Can techniques used to detect fish in ADCP data complement and improve current fish detection methods? The ADCP provides an alternative processing approach for dealing with near-surface bubbles that eliminates the need for the more operator intensive process of determining an entrained air exclusion line.

3. Can this fish detection algorithm and package be used to calculate fish count in other ADCP data? If the broadband ADCP data is unaveraged, i.e. one ping per ensemble, then the BAMFF package can be used to extract fish counts, fish school velocities and water velocities.

6.1.1 Relevance to the field

Holliday (1977), Olsen et al. (1983), and Demer (2000) all saw the potential for velocity measurements of fish with Doppler shift instruments, and identified technology advancements and data processing methods as outstanding challenges. Broadband technology produces a more precise measurement by using autocorrelation to calculate velocity. Conveniently, the autocorrelation provides a measure of the quality of the backscattered signal [Tollefsen and Zedel, 2003]. This development is a critical turning point in developing the capabilities of fish detection with ADCP because it can differentiate fish targets from regions of continuous volume backscatter, such as water or bubble plumes. Additionally, Zedel and Cyr-Racine (2009) remove the dependence on assuming the bins have homogeneous flow and have developed a data processing method that uses an optimization algorithm to extract both the fish and water velocities. Both of these developments to Doppler shift measurements enable the detection of fish using broadband ADCPs. The effect of the development of the correlation threshold has been shown in Figure 4.2, through the identification of fish targets in the fish school using intensity and correlation thresholds. The advancement in fish and water velocity extraction through a least-squares algorithm can be used in tandem with the fish detection method to extract fish velocities from ADCP data.

Understanding the algorithm and code that converted and calibrated the raw ADCP data used when detecting fish was a priority throughout this research. A thorough understanding of the code, its inner workings and purpose, was required to convert it into an approachable package with clear documentation. The BAMFF

package collects all the required components to advance the field of fish detection with broadband Doppler sonar and makes the methods more broadly accessible. The results of this research can be used for various future deployments, and even previous ones. Not only is this work relevant for high energy tidal channels, but anywhere a broadband ADCP is deployed and there is interest in the fish count and fish velocity, in addition to the water velocity.

The developments suggested here can be of use at sites identified as having the potential for in-stream tidal turbines. Both Melvin and Cochrane (2014) and Viehman and Zydlewski (2017) had ADCPs deployed at their study sites for water velocity measurements. Fish monitoring in these areas can benefit from the ADCP's ability to detect fish in bubble plumes and the ease at which they can be deployed for longer periods. ADCP fish detection provides the ability to know when to expect fish and at what depth. This ability is shown in Figure 5.1 where fish counts over time and depth are comparable with the split-beam results. Nonetheless, split-beam echosounders can not be replaced with ADCPs, as split-beam echosounders report information on target strength and are used to understand species composition. However, the ADCP data can be used in tandem with split-beam echosounders for longer time series, confirmation of results, velocity measurements of fish schools and detections in entrained air.

6.2 Future Work

There are three main components to the research presented in this thesis that could benefit from a deeper exploration: using the BAMFF package on other datasets, determining the optimal intensity and correlation thresholds and validating the ADCP fish velocities.

The BAMFF package has yet to be used on previously collected broadband ADCP data sets that are unaveraged. An existing year-long time series of Grand Passage collected in 2012 will be a good place to start for this analysis. The new capabilities of broadband ADCP systems can add value to time series that have already been collected and processed for water velocity measurements. It would be an interesting avenue of research to explore the fish detections and velocity in long ADCP time series that had the initial purpose of only measuring water velocities.

A systematic approach to choosing the thresholds for the BAMFF fish detection algorithm could give a deeper understanding of the effect of different thresholds on fish detections. The correlation and intensity threshold values were determined by trial and error until fish were detected in fish schools without false detections in bubbles. An in-depth sensitivity analysis of the thresholds would clarify their relationship to the medium (fish, bubble or water), the data collection parameters and each other.

Due to the unexpected lack of fish during the second deployment, the ADCP determined fish velocities have yet to be validated. The methods used in this thesis

would be adequate for a fish velocity comparison between the least-squares method of the ADCP data and fish tracking with a split-beam echosounder. It has been verified that the least-squares approach agrees with the conventional processing method for water velocities [Zedel and Cyr-Racine, 2009]. As with the water velocities, the velocities of fish school are expected to be correctly calculated, assuming there is enough fish present. A comparison with split-beam tracking methods could provide a chance to enhance some of the methods used in multiple target tracking, such as situations when individual fish cannot be isolated.

In conclusion, the research presented in this thesis expands the ability of broadband ADCPs. It has been shown that ADCPs have the ability to detect fish in agreement with split-beam echosounder results and to detect fish in entrained air, a task split-beam echosounders are unable to complete with standard fish tracking algorithms. These additional abilities are useful but echosounders remain indispensable for fisheries research of TS-length relationship and species compositions studies. These findings are relevant for stock assesment studies over long time periods. Long time series are essential for monitoring fish populations through the rapid changes in ocean temperature, habitat and fish populations.

Bibliography

[Balk and Lindem, 2017] Balk, H. and Lindem (2017). Sonar4 and sonar5-pro post-processing systems, operator manual version 604, cageeye as.

[Balk and Lindem, 2002] Balk, H. and Lindem, T. (2002). A new method for single target detection.

[BioSonics, 2016] BioSonics (2016). Dt-x submersible quick start guide.

[Blackman, 1986] Blackman, S. S. (1986). *Multiple-target tracking with radar applications*. Dedham, MA, Artech House, Inc., 1986, 463 p.

[Broadhurst et al., 2014] Broadhurst, M., Barr, S., and Orme, C. D. L. (2014). In-situ ecological interactions with a deployed tidal energy device; an observational pilot study. *Ocean & coastal management*, 99:31–38.

[Demer et al., 2000] Demer, D. A., Barange, M., and Boyd, A. J. (2000). Measurements of three-dimensional fish school velocities with an acoustic Doppler current profiler. *Fisheries Research*, 47(2-3):201–214.

[Ehrenberg and Torkelson, 1996] Ehrenberg, J. E. and Torkelson, T. C. (1996). Application of dual-beam and split-beam target tracking in fisheries acoustics. *ICES Journal of Marine Science*, 53(2):329–334.

[Enzenhofer et al., 1998] Enzenhofer, H. J., Olsen, N., and Mulligan, T. J. (1998). Fixed-location riverine hydroacoustics as a method of enumerating migrating adult Pacific salmon: comparison of split-beam acoustics vs. visual counting. *Aquatic Living Resources*, 11(2):61–74.

[Foote, 1982] Foote, K. G. (1982). Optimizing copper spheres for precision calibration of hydroacoustic equipment. *The Journal of the Acoustical Society of America*, 71(3):742–747.

[Foote, 1983] Foote, K. G. (1983). Linearity of fisheries acoustics, with addition theorems. *The Journal of the Acoustical Society of America*, 73(6):1932.

[Foote et al., 1986] Foote, K. G., Aglen, A., and Nakken, O. (1986). Measurement of fish target strength with a split-beam echo sounder. *The Journal of the Acoustical Society of America*, 80(2):612–621.

[Fraser et al., 2017] Fraser, S., Nikora, V., Williamson, B. J., and Scott, B. E. (2017). Automatic active acoustic target detection in turbulent aquatic environments. *Limnology and Oceanography: Methods*, 15(2):184–199.

[Freitag et al., 1993] Freitag, H. P., Plimpton, P. E., and McPhaden, M. J. (1993). Evaluation of an adcp fish-bias rejection algorithm. In *Proceedings of OCEANS'93*, pages II394–II397. IEEE.

[Holliday, 1977] Holliday, D. V. (1977). Two applications of the doppler effect in the study of fish schools. *Rapports et Proces-verbaux des Réunions. Conseil International pour l'Éxploration de la Mer*, 170:21–30.

[Instruments, 2001] Instruments, R. (2001). Workhorse sentinel adcp user's guide.

[Korneliussen, 2018] Korneliussen, R. J. (2018). Acoustic target classification.

[Maclennan et al., 2002] Maclennan, D. N., Fernandes, P. G., and Dalen, J. (2002). A consistent approach to definitions and symbols in fisheries acoustics. *ICES Journal of Marine Science*, 59(2):365–369.

[MacLennan and Simmonds, 2013] MacLennan, D. N. and Simmonds, E. J. (2013). *Fisheries acoustics*, volume 5. Springer Science & Business Media.

[McTamney, 2019] McTamney, A. (2019). Detecting wild fish and zooplankton near fish farms during and after fallow periods in southern newfoundland. Master's thesis, Memorial University of Newfoundland.

[Medwin and Clay, 1997] Medwin, H. and Clay, C. S. (1997). *Fundamentals of acoustical oceanography*. Academic press.

[Melvin and Cochrane, 2014] Melvin, G. D. and Cochrane, N. A. (2014). *Investigation of the Vertical Distribution, Movement and Abundance of Fish in the Vicinity of Proposed Tidal Power Energy Conversion Devices*. Number October 2012.

[Miyanohana et al., 1993] Miyanohana, Y., Ishii, K., and Furusawa, M. (1993). Spheres to calibrate echo sounders at any frequency. *BULLETIN-JAPANESE SOCIETY OF SCIENTIFIC FISHERIES*, 59:933–933.

[Mullison, 2017] Mullison, J. (2017). Backscatter estimation using broadband acoustic doppler current profilers-updated. In *Proceedings of the ASCE Hydraulic Measurements & Experimental Methods Conference, Durham, NH, USA*, pages 9–12.

[Olsen et al., 1983] Olsen, K., Angel, J., Pettersen, F., Løvik, A., Nakken, O., Venema, S., et al. (1983). Observed fish reactions to a surveying vessel with special reference to herring, cod, capelin and polar cod.

[SAFT, 2010] SAFT (2010). *Technical Data Sheet LS 33600*.

[Shen et al., 2016] Shen, H., Zydlewski, G. B., Viehman, H. A., and Staines, G. (2016). Estimating the probability of fish encountering a marine hydrokinetic device. *Renewable Energy*, 97:746–756.

[Staines et al., 2015] Staines, G., Zydlewski, G., Viehman, H., Shen, H., and McCleave, J. (2015). Changes in vertical fish distributions near a hydrokinetic device in cobscook bay, maine, usa. In *Proceedings of the 11th European Wave and Tidal Energy Conference (EWTEC2015), Nantes, France*, pages 6–11.

[Tollefsen and Zedel, 2003] Tollefsen, C. D. and Zedel, L. (2003). Evaluation of a doppler sonar system for fisheries applications. *ICES Journal of Marine Science*, 60(3):692–699.

[Trenkel et al., 2019] Trenkel, V., Vaz, S., Albouy, C., Amour, A. B., Duhamel, E., Laffargue, P., Romagnan, J., Simon, J., and Lorance, P. (2019). We can reduce the impact of scientific trawling on marine ecosystems. *Marine Ecology Progress Series*, 609:277–282.

[Vent et al., 1976] Vent, R. J., Davies, I. E., Townsen, R. W., and Brown, J. C. (1976). Fish school target strength and Doppler measurements. Technical report, NAVAL UNDERSEA CENTER SAN DIEGO CA.

[Viehman and Zydlewski, 2015] Viehman, H. A. and Zydlewski, G. B. (2015). Fish interactions with a commercial-scale tidal energy device in the natural environment. *Estuaries and Coasts*, 38(1):241–252.

[Viehman and Zydlewski, 2017] Viehman, H. A. and Zydlewski, G. B. (2017). Multi-scale temporal patterns in fish presence in a high-velocity tidal channel. *PloS one*, 12(5):e0176405.

[Viehman et al., 2015] Viehman, H. A., Zydlewski, G. B., McCleave, J. D., and Staines, G. J. (2015). Using hydroacoustics to understand fish presence and vertical distribution in a tidally dynamic region targeted for energy extraction. *Estuaries and Coasts*, 38(1):215–226.

[Xie et al., 1997] Xie, Y., Conkite, G., and Mulligan, T. (1997). A split beam echosounder perspective on migratory salmon in the Fraser River: a progress report on the split-beam experiment at Mission, B.C. in 1995. *Pacific Salmon Commission Technical Report*, 8:pp. 32.

[Zedel and Cyr-Racine, 2009] Zedel, L. and Cyr-Racine, F.-Y. (2009). Extracting fish and water velocity from doppler profiler data. *ICES Journal of Marine Science*, 66(9):1846–1852.

[Zedel et al., 2019] Zedel, L., Dunn, M., Cyr-Racine, F.-Y., and Cameron, H. (2019). Bamff: Broadband acoustic monitoring for fish.

Appendix A

BAMFF Documentation

Included here is the landing page of the BAMFF package documentation webpage (Figure A.1). The full website containing a literature review, algorithm documentation, a quick start guide and references can be accessed at www.bamff.readthedocs.io.

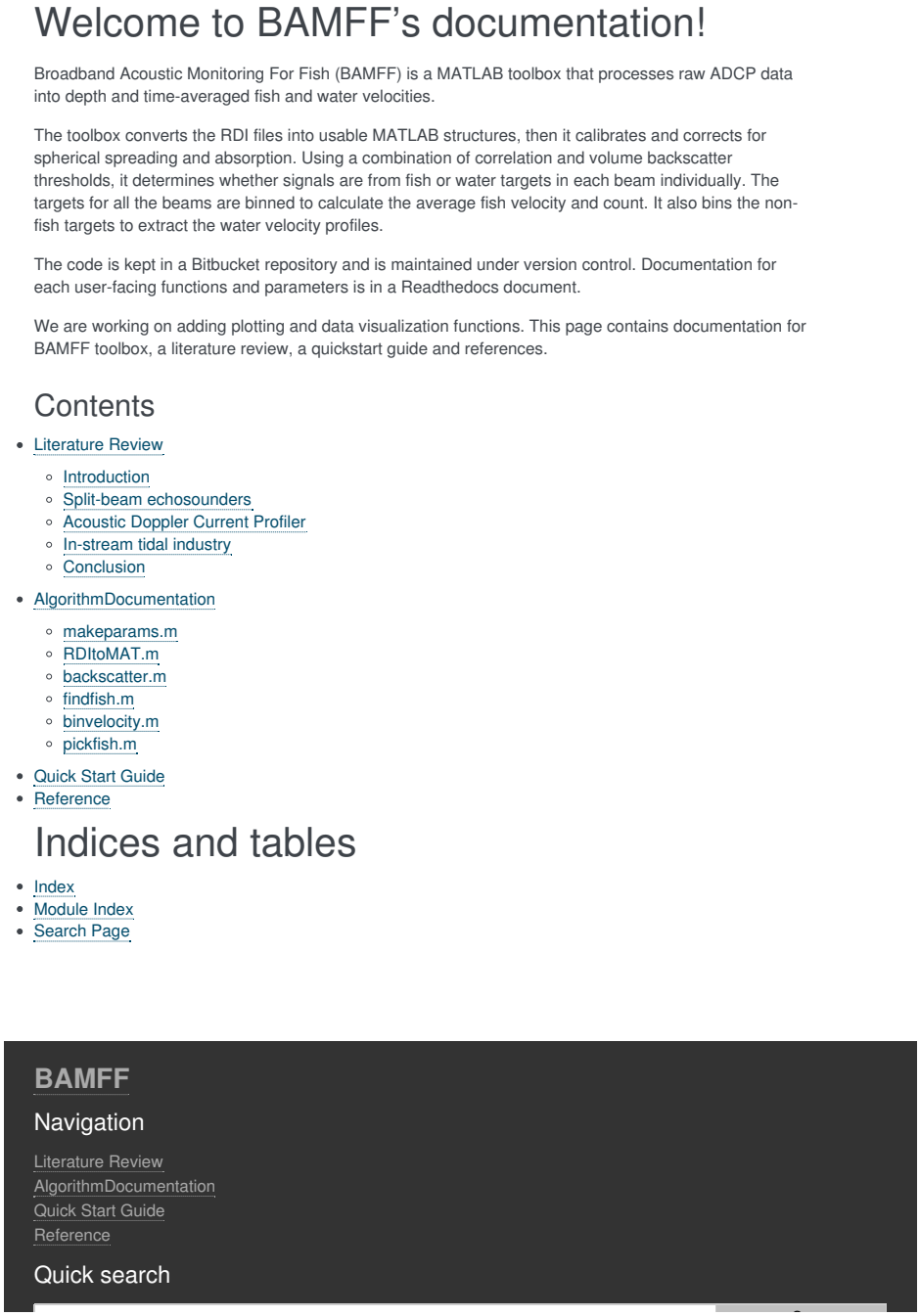

Figure A.1: The landing page of the Broadband Acoustic Monitoring For Fish (BAMFF) package documentation at www.bamff.readthedocs.io